ANL/ET/CP--92179
CONF-971115--

FLUID-DAMPING-CONTROLLED INSTABILITY OF TUBES IN CROSSFLOW

S. S. Chen and Y. Cai
Energy Technology Division
Argonne National Laboratory
Argonne, Illinois

and

G. S. Srikantiah
Nuclear Power Division
Electric Power Research Institute
Palo Alto, California

Submitted for presentation at the ASME International Mechanical Engineering Congress and Exposition, November 16-21, 1997, Dallas, Texas.

*Work supported by Electric Power Research Institute under an agreement with the U.S. Department of Energy, Contract Agreement 31-109-Eng-38-85989.

DISCLAIMER

ABSTRACT

A mathematical model for fluid-damping-controlled instability of tubes presented in this paper is based on the unsteady flow theory. Motion-dependent fluid forces are measured in a water channel. From the measured fluid forces, fluid-stiffness and fluid-damping coefficients, are calculated as a function of reduced flow velocity, oscillation amplitude, and Reynolds number. Once these coefficients are known, the mathematical model can be applied to predict structural instability due to fluid damping. Many cases are considered: single tube, twin tubes, tube row, triangular array, and square arrays. The results show the instability regions based on the fluid damping coefficients and provide the answers to a series of questions on fluidelastic instability of tube arrays in crossflow.

1. INTRODUCTION

Several theories have been used to study the vibration and stability of tubes in crossflow, quasistatic, quasisteady, and unsteady flow theories (Chen 1987a & 1987b, Price 1993). In some parameter ranges, both quasistatic and quasisteady flow theories have certain advantages because of the simplicity in obtaining motion-dependent fluid forces. However, only the unsteady flow theory can be applied in any range of parameters. In this study, the unsteady flow theory is used.

One of the frequently asked question is the stability of a flexible tube among a rigid tube array subjected to crossflow. In the original stability criterion developed by Connors (1970) about a quarter century ago, at least two flexible tubes are needed to have fluidelastic instability. In the case considered by Connors, the instability was due to fluid-stiffness-controlled instability and a minimum of two

degrees of freedom are needed. Tests by various experimentalists found that a single flexible among tube arrays show instability in some cases while it is stable in other cases (Chen 1983a, Price et al. 1986, Price and Paidoussis 1987). Chen (1983a and 1983b) about 15 years ago developed a mathematical model based on the measured motion-dependent fluid forces by Tanaka and his colleagues (Tanaka 1980, Tanaka and Takahara 1981, Tanaka et al. 1982) to characterize the difference of the two mechanisms which provide the theoretical basis of the occurrence of different stability mechanisms. In the past, because of the limited amount of fluid-force coefficient data available, the theory can not provide quantitative answer on the stability of tubes in various situations.

Recently, extensive tests of motion-dependent fluid forces have been performed (Chen et al. 1994, 1995, 1996, Zhu et al. 1995, 1996). Using the unsteady fluid forces and unsteady flow theory, it will provide some answers to the frequently asked questions on fluidelastic instability. The purpose of this paper is study fluid-damping-controlled instability of tubes in different situations.

2. UNSTEADY FLOW THEORY

Consider a tube oscillating in crossflow as shown in Fig. 1. The tube may stand alone or surrounded by other rigid tubes. The fluid is flowing at velocity U. When the tube is held stationary, it is subjected to drag and lift forces. The displacement components of the tube in the x and y directions are u and v, respectively. Once the tube starts to move, additional fluid forces, called motion-dependent fluid forces, will be induced due to tube motion. The motion-dependent fluid-force components per unit length that act on the tube in the x and y directions are f and g, respectively, and are given (Chen 1987a and 1987b) as

$$f = -\rho\pi R^2\left(\alpha\frac{\partial^2 u}{\partial t^2}+\sigma\frac{\partial^2 v}{\partial t^2}\right)+\frac{\rho U^2}{\omega}\left(\alpha'\frac{\partial u}{\partial t}+\sigma'\frac{\partial v}{\partial t}\right)+\rho U^2(\alpha'' u+\sigma'' v), \tag{1}$$

$$g = -\rho\pi R^2\left(\tau\frac{\partial^2 u}{\partial t^2}+\beta\frac{\partial^2 v}{\partial t^2}\right)+\frac{\rho U^2}{\omega}\left(\tau'\frac{\partial u}{\partial t}+\beta'\frac{\partial v}{\partial t}\right)+\rho U^2(\tau'' u+\beta'' v) \tag{2}$$

where ρ is fluid density, R is tube radius, t is time, and ω is circular frequency of tube oscillations. α, β, σ, and τ are added mass coefficients, α', β', σ', and τ' are fluid-damping coefficients, and α'', β'', σ'', and τ'' are fluid-stiffness coefficients.

Various methods can be used to measure fluid-force coefficients. In this study, the unsteady flow theory is used. Fluid-force coefficients can be determined by measuring the fluid forces acting on the tube as a result of its oscillations. If the tube is excited in the x direction, its displacement in the x direction is given by

$$u = d_o \cos \omega t, \tag{3}$$

where d_o is the oscillation amplitude. The motion-dependent fluid-force components acting on the tube in the x and y directions are

$$f = \frac{1}{2}\rho U^2 e_\ell \cos(\omega t + \phi_\ell) d_o \tag{4}$$

$$g = \frac{1}{2}\rho U^2 e_d \cos(\omega t + \phi_d) d_o, \tag{5}$$

where e_ℓ and e_d are the fluid-force amplitudes and ϕ_ℓ and ϕ_d are the phase angles by which the fluid forces acting on the tube lead the displacement of the tube.

By using Eqs. 1-3, we can also write the fluid-force components as

$$f = \left(\rho\pi R^2\omega^2\alpha + \rho U^2\alpha''\right)d_o \cos\omega t - \rho U^2\alpha' d_o \sin\omega t \tag{6}$$

$$g = \left(\rho\pi R^2\omega^2\tau + \rho U^2\tau''\right)d_o \cos\omega t - \rho U^2\tau' d_o \sin\omega t. \tag{7}$$

Using Eqs. 4 and 6 and Eqs. 5 and 7 yields

$$\begin{aligned}
\alpha'' &= \frac{1}{2}e_\ell \cos\phi_\ell - \frac{\pi^3}{Ur^2}\alpha \\
\tau'' &= \frac{1}{2}e_d \cos\phi_d - \frac{\pi^3}{Ur^2}\tau \\
\alpha' &= \frac{1}{2}e_\ell \sin\phi_\ell \\
\tau' &= \frac{1}{2}e_d \sin\phi_d,
\end{aligned} \tag{8}$$

where Ur is the reduced flow velocity ($Ur = \pi U/\omega R$). The added mass coefficients α and τ can be calculated from the potential flow theory (Chen 1987a). They can also be measured directly from the excitation of the tube in stationary fluid. Other fluid-force coefficients, β', β'', σ', and σ'', can be obtained in a similar manner by exciting the tube in the y direction.

3. MOTION-DEPENDENT FLUID-FORCE COEFFICIENTS

A water channel was used to measure motion-dependent fluid forces. The test setup and measurement technique are presented in an earlier paper (Chen et al. 1994).

Many cases were considered in this study (Fig. 2). Different tube arrays are described by the tube pitch in the drag direction P and lift direction T and tube diameter D (D = 2.54 cm).

- Case a - Single Tube: The tube was located in the middle of the water channel. Various flow velocities were tested, 0.064, 0.11, and 0.127 m/s. The tube was excited to various oscillation amplitudes in the lift direction.

- Case b - Two Tubes Normal to Flow: T/D = 1.35. Five flow velocities were tested, 0.05, 0.07, 0.113, 0.146, and 0.166 m/s. The tube is excited in the lift and drag directions.

- Case c - Two Tubes in Tandem: P/D = 1.35 (Case c.1), 2.70 (Case c.2), and 4.05 (Case c.3). For Case c.1, the upstream tube was excited at three flow velocities in the lift and drag directions, 0.07, 0.11, and 0.15 m/s. For the downstream tube in Cases c.1, c.2, and c.3, the flow velocity was set at 0.11 m/s and the excitation amplitude was set to various values.

- Case d - A Tube in the Wake of Another Rigid Tube: Three cases are tested: Case d.1- P/D = 2.7, T/D = 1.35; Case d.2, P/D = 4.05, T/D = 1.35; and Case d.3, P/D = 4.05, T/D = 2.70. The flow velocity was set at 0.11 m/s and the excitation amplitude was set to various values.

- Case e - Tube Row: T/D = 1.35 (Case e.1) and 2.7 (Case e.2). Four flow velocities, 0.063, 0.092, 0.125, and 0.131 m/s, were set for Case e.1. The flow velocity was set at 0.11 m/s and the excitation amplitude was set to various values for Case e.2.

- Case f - Triangular Array: T/D = 1.35. The tube may be located in the upstream (Case f.1), middle (Case f.2), and downstream (Case f.3) of the tube array. Tests were performed at U = 0.07, 0.11, and 0.16 m/s.

- Case g - Square Array with P/D = T/D = 1.35: The tube may be located in the upstream (Case g.1), middle (Case g.2, Case g.3), and downstream (Case g.4) of the tube array corresponding to 1, 2, 3, and 4 shown in Fig. 2.2. Tests were performed at U = 0.1 m/s and tests were repeated for each case.

- Case h - Square Array with P/D = T/D = 1.42: The tube was located in the middle of the tube array. The flow velocities were set at 0.06, 0.11, and 0.16 m/s.

- Case i - Square Array with P/D = T/D = 1.46: The tube may be located in the upstream (Case i.1), middle (Case i.2), and downstream (Case i.3) of the tube array. Two flow velocities were tested for Case i.1 (U = 0.11 and 0.165 m/s) and Case i.3 (U = 0.125 and 0.18 m/s) and three flow velocities were tested for Case c.2 (U = 0.06, 0.11, and 0.16 m/s).

The flexible tube in various cases was excited in the lift (x) or drag (y) direction, with a displacement $u(t) = d_0 \cos \omega t$. The fluid forces acting on the tube f(t) and g(t) are measured simultaneously with the displacement. From the time histories of fluid forces, fluid-damping coefficients, α' and τ', and fluid-stiffness coefficients α'' and τ'', were calculated from Eqs. 8 and similar equations for β', σ', β'', and σ'' in the drag direction.

Fluid-force coefficients are a function of flow velocity, excitation frequency, and excitation amplitude. In each case, when the flow velocity is set at a specific

value, the tube is excited at a frequency (0.2-2.0 Hz) with a series of amplitudes d (0.6-3.5 mm), where d is the RMS value of u(t), given in Eq. 3. Reynolds number Re varied from about 1500-4500 based on the gap velocity U.

Figures 3-15 show the experimentally determined fluid-force coefficients. All fluid-force coefficients were plotted as a function of reduced flow velocity Ur (= U/fD; U = gap velocity, f = $\omega/2\pi$, D = tube diameter). The following general characteristics of the fluid-force coefficients were observed:

- At high reduced flow velocity, the coefficients were almost independent of reduced flow velocity and excitation amplitude. This characteristic is similar for all tube arrays and other geometries (Chen 1987b). Therefore, at high reduced flow velocity, the fluid-force coefficients are much easier to quantify. Once, they are determined at a specific set of parameters, they can be applied to various values of flow velocity, excitation frequency, and excitation amplitude.

- Drastic changes in the fluid-force coefficients occurred in the region at low reduced flow velocity (Ur < 10).

- In the critical region corresponding to the lower reduced flow velocity, the magnitudes of the coefficients also depend on the excitation amplitude.

The following additional characteristics were noted for each case.

Single Tube (Figs. 3 and 4)

From Figs. 3 and 4 as well as additional data not included here, α' is positive for Ur varying from about 5 to 11 and its value decreases with excitation amplitude. The range depends on Reynolds number and oscillation amplitude.

Reynolds Number: At lower Re, α' become positive at lower Ur. At higher Re, α' becomes positive at higher Ur. However, its range varies from about 4.8 to 5.4. As Ur is increased, α' becomes negative again.

Oscillation Amplitude: At lower oscillation amplitude, α' become positive at lower Ur. At higher oscillation amplitudes, α' becomes positive at higher Ur. However, its range also depends on Re. As Ur is increased, the effect of oscillation amplitude is small.

The value of α'' is positive for smaller Ur and becomes negative as Ur is increased. The crossing point varies from Ur equal to 5.4 to 6. At high reduced flow velocity, both α' and α'' are approximately independent of Re, Ur, and oscillation amplitude. The values of Ur corresponding to the peak values of α' and α'' increase with the excitation amplitude and Re, and the peak values of α' and α'' were approximately the same for various values of Re.

Two Tubes Normal to Flow (Fig. 5)

β' is always negative throughout the whole range of Ur. α' is negative at lower Ur; its range depends on Reynolds number. Comparing Fig. 5 with Fig. 3, the region for negative α' is at lower Ur for Case b. As Reynolds number increases, the region of negative α' shifts to higher Ur and its range increases

slightly. However, the peak magnitude of α' decreases with Re. This is similar to that of a single tube as shown in Fig. 3.

Two Tubes in Tandem (Figs. 6 and 7)

In Case c.1, α' becomes positive as soon as Ur reaches a certain value which is equal to 6 to 7 for the tube in the upstream, Fig. 6. The precise crossing point depends on Re and α' continues to be positive at high Ur (in this case, test has been performed for Ur up to 60). On the other hand, β' is always negative for all Ur.

When the tube is in the downstream of another tube, the force coefficients are given in Fig. 7. α' is positive at lower Ur while β' is negative only in a small range. As P/D increases, the magnitude of α' decrease and the region of positive α' shifts to larger Ur.

A Tube in the Wake of Another Tube (Figs. 8a and 8b)

The general characteristics of α', α'', β', and β'' are similar for the tube located at three different positions in the wake of the upstream tubes. β' and β'' are negative in the reduced flow velocity range tested. However, α' is positive at the lower reduced flow velocity. The peak values of α' depend on the location and it value can be much larger than that of a single tube.

Tube Row (Figs. 9-11)

The general trend of α' and α'' in Cases e.1 and e.2 are similar to those of a single tube. However, the region of positive α' for Case e.1 is at lower reduced flow velocity. This can be seen clearly from Fig. 9. At lower Re, the effects of

oscillation amplitude appear to be smaller than those for the larger Re. In Case e.2, the pitch-to-diameter ratio is much larger and the general characteristics of α' and α'' are about the same as those of a single tube.

Triangular Array (Figs. 12a and 12b)

Damping coefficients α' and β' shown in Figs. 12a and 12b show that in Cases f.1 and f.2 when the tube is in the upstream and middle of tube array, they are negative at all reduced flow velocity. The only case in which α' becomes positive is at low reduced flow velocity in Case f.3 when the tube is in the downstream. The general trend of α', β', and β'' as a function of reduced flow velocity are similar for the three cases.

Square Arrays (Figs. 13, 14, and 15)

Figures 13-15 show that fluid force coefficients, α', α'', β', and β'', depend on pitch-to-diameter ratio and tube location.

- β' is positive for the tube at any location and regardless of pitch-to-diameter ratio.

- α'' and β'' are similar for the tube at various location and different pitch-to-diameter ratio.

- α' depends on tube location and pitch-to-diameter ratio. When the tube is upstream, α' is negative except at very small Ur. At large Ur, it is always positive. The crossing point from negative to positive values depends on Reynolds number, pitch-to-diameter ratio, and tube location. For a fixed Reynolds number, the crossing point of α' from negative to

positive is the smallest for the upstream tube and the largest for the downstream tube. This can be seen clearly from Fig. 15a.

4. FLUID-DAMPING-CONTROLLED INSTABILITY

Once motion-dependent fluid forces are known, the response of the tube can be predicted. As an example, consider a single tube supported by springs. The tube is subjected to a crossflow uniformly along its length ℓ. The equation of motion in the lift direction is

$$m\frac{d^2u}{dt^2}+C\frac{du}{dt}+Ku+\frac{\rho\pi D^2}{4}\alpha\frac{d^2u}{dt^2}-\frac{\rho U^2}{\omega}\alpha'\frac{du}{dt}-\rho U^2\alpha'' u=\frac{1}{2}\rho U^2 D C_L' \cos(\omega_s t), \quad (9)$$

where K is the spring constant, C is the tube damping coefficient, m is the tube mass per unit length, C is the fluctuating lift coefficient and ω_s is the circular frequency of vortex shedding.

The in-vacuum variables, i.e., natural frequency f_v and modal damping ratio ζ_v, can be calculated from the equation of motion or from an in-vacuum test (practically in air). Let

$$u(z,t) = Dq(t),$$

$$Ur=\frac{U}{fD}, \quad (10)$$

$$\gamma=\frac{\rho\pi D^2}{4m},$$

where f is oscillation frequency and U is gap velocity. Substituting Eqs. 10 in Eq. 9, one obtains

$$\frac{d^2q}{dt^2}+2\zeta\omega\frac{dq}{dt}+\omega^2q=\frac{1}{2(1+\gamma\alpha)}\left(\frac{\rho U^2C_L'}{m}\right)\cos(\omega_s t), \tag{11}$$

where

$$\omega=\omega_v(1+\gamma C_M)^{-0.5},$$

$$\zeta=\frac{\zeta_v}{1+\gamma\alpha}\left[(1+\gamma C_M)^{0.5}-\frac{\gamma Ur^2\alpha'}{2\zeta_v\pi^3}\right], \tag{12}$$

$$C_M=\alpha+\frac{Ur^2\,\alpha''}{\pi^3}.$$

Note that ω and ζ are the circular frequency and modal damping ratio, respectively, for the tube in crossflow. C_M is called an added mass coefficient for the tube in flow; when Ur = 0, it is equal to α. When $Ur \neq 0$, C_M depends on Ur as well as on α'', which in turn, depends on Ur and oscillation amplitude.

For motion in the drag direction, Eqs. 11 and 12 are applicable as long as the fluid force coefficients α, α', and α'', are replaced by β, β', and β'', and the lift coefficient C_L' and vortex shedding frequency ω_s are replaced by C_D' and $2\,\omega_s$ respectively. The system response due to vortex shedding and other excitation can be obtained by solving Eq. 11. Note that inasmuch as the fluid-force coefficients α' and α'' are a function of Ur, the natural frequency ω and modal damping ratio ζ are a function of the reduced flow velocity Ur. The unsteady flow theory can form the basis for calculating a complete response due to flow. The calculation will require an iteration technique.

When modal damping becomes negative, the tube becomes dynamically unstable and high-amplitude oscillations will develop. As the oscillation amplitude increases, other nonlinear effect may become important and the system may be stabilized. The critical flow velocity of dynamic instability can be calculated from

$$\zeta = 0. \tag{13}$$

From Eqs. 12 and 13, the critical reduced flow velocity at which the modal damping ratio is zero can be calculated from

$$Ur = 4\sqrt{2\pi}\left(\frac{\delta}{\alpha'}\right)^{0.5}\left[\frac{\delta}{\pi^2}\left(\frac{\alpha''}{\alpha'}\right) \pm \sqrt{\left(\frac{\delta}{\pi^3}\frac{\gamma\alpha''}{\alpha'}\right)^2 + \frac{1+\gamma\alpha}{4}}\right]^{0.5}, \tag{14}$$

where δ is a mass-damping parameter ($\delta = 2\pi\,\zeta_v\, m/\rho D^2$). This is the critical flow velocity for fluidelastic instability in the lift direction. Similarly, the critical flow velocity for motion in the drag direction is

$$Ur = 4\sqrt{2\pi}\left(\frac{\delta}{\beta'}\right)^{0.5}\left[\frac{\delta}{\pi^2}\left(\frac{\beta''}{\beta'}\right) - \sqrt{\left(\frac{\delta}{\pi^3}\frac{\gamma\beta''}{\beta'}\right)^2 + \frac{1+\gamma\beta}{4}}\right]^{0.5}. \tag{15}$$

From Eqs. 14 and 15, the critical flow velocity for fluid-damping-controlled can be calculated. Since α', β, α'', and β'' depend on Ur, the calculation requires an iteration process.

5. DISCUSSIONS AND NUMERICAL EXAMPLES

The modal damping ratio given in Eq. 12 shows that it consists of two parts, tube damping and fluid damping. Tube damping is always positive while fluid

damping may be positive or negative. In order to make the total damping ratio, α' or β' must be positive. Based on the fluid-force coefficients given in Figs. 3 to 15, the potential instability regions are summarized in Table 1.

From Table 1, several conclusions are noted:

- The motion in the drag direction is much more stable. Practically it will not become unstable by fluid-damping-controlled instability in the drag direction for various tube arrays.

- For triangular array, fluid-damping-controlled instability is not possible for the upstream tube and tube in the middle of tube array because the fluid-damping coefficients α' and β' are negative.

- For the upstream tube of two tubes in tandem and the upstream tube or tube in the middle of a square tube array, once the reduced flow velocity reaches a certain values, the damping coefficient α' becomes positive.

The effects of several parameters on the fluid-damping coefficient, α'', are considered in detail:

Table 1. Regions with positive α' and β' in which fluidelastic instability may occur

Cases	Pitch-to-Diameter Ratio	Lift Direction	Drag Direction
a (single tube)		5 < Ur < 11	Not Measured
b (two tubes normal to flow)	T/D = 1.35	2 < Ur < 6	None
c.1 (two tubes in tandem) Upstream Tube	P/D = 1.35	7 < Ur	None
c.1 (two tubes in tandem) Downstream Tube	P/D = 1.35	3.5 < Ur < 8	2.2 < Ur < 3.6
c.2 (two tubes in tandem) Downstream Tube	P/D = 2.70	3.6 < Ur < 7.4	None
c.2 (two tubes in tandem) Downstream Tube	P/D = 4.05	5.3 < Ur < 20	None
d.1 (a tube in the wake of another tube)	P/D = 2.7 T/D = 1.35	4.2 < Ur < 10	None
d.2 (a tube in the wake of another tube)	P/D = 4.05 T/D = 1.35	5.2 < Ur < 9.5	None
d.3 (a tube in the wake of another tube)	P/D = 4.05 T/D = 2.7	4.7 < Ur < 9.3	None
e.1 (tube row)	T/D = 1.35	1.1 < Ur < 4.0	None
e.2 (tube row)	T/d = 2.70	5 < Ur < 9.5	None
f.1 (triangular array) Upstream Tube	P/D = 1.35	Ur > 25	None
f.2 (triangular array) Middle of Tube Array	P/D = 1.35	None	None
f.3 (triangular array) Downstream Tube	P/D = 1.35	1.5 < Ur < 5.5	Ur > 30 (Re = 1760) Ur > 50 (Re = 2760) Ur > 62 (Re = 4010)
g.1 (square array) Upstream Tube	P/D = 1.35	1.5 < Ur	None
g.2 (square array) 2nd Row of Tube	P/D = 1.35	2.0 < Ur	None
g.3 (square array) 2nd Row from Downstream Tube	P/D = 1.35	2.0 < Ur	None
g.4 (square array) Downstream Tube	P/D = 1.35	2 < Ur < 6	None
h (square array) Middle of Tube Array	P/D = 1.42	1.5 < Ur	None
i.1 (square array) Upstream Tube	P/D = 1.46	1.7 < Ur	None
i.2 (square array) Middle of Tube Array	P/D = 1.46	2.1 < Ur	None
i.3 (square array) Downstream Tube	P/D = 1.46	3.1 < Ur < 7	None

1. Tube Location

Fluid-force coefficient, α', depends on tube location in a square array (P/D = 1.46). As an example, Fig. 16 shows α' for tube at upstream, middle, and downstream of tube array. When Ur reaches a certain value, α' becomes positive. The crossing point depends on tube location. The sequence is upstream, middle, and downstream tubes. At high Ur, the middle tube has positive α' for all large Ur while for the upstream and downstream tubes, they become very small and become negative again. Based on α', it can be seen that in a square array, the upstream tube will become unstable first and then the middle tube and finally the downstream tube. This was noticed in an earlier experiment of square array (Chen and Jendrzejczyk 1981, Chen 1984). For the middle tube, the instability will be sustained throughout all Ur. The effect of tube location for triangular arrays can be seen in Fig. 12a; the downstream tube can become unstable.

2. Tube Pitch

Fluid-force coefficients depend on pitch-to-diameter ratio. Figure 17 shows α' for three different values of P/D (1.35, 1.42, and 1.46) for square array. For the upstream and middle tubes, the crossing point of α' is almost independent of P/D while the downstream tube is approximately the same as that of a tube row (Chen et al. 1994). The value of α' at high Ur for the upstream and middle of tube arrays do depend on P/D. For the downstream tube, the effect is much smaller. This is consistent with the previous data on fluidelastic instability of square arrays.

3. Downstream Tube

Figure 18 shows α' for various tube array with P/D = 1.35. In all cases, at lower Ur corresponding to vortex shedding region, α' is positive. The location and the range depend on tube array. The single tube occurs at higher Ur while tube arrays occurs at lower Ur. The peak value of α' is the largest for tube row, then triangular tube array, and finally square array and two tube normal to flow. It is also noted that the first crossing point of α' for all tube arrays are very close to each other. Another characteristic is that the crossing point of α' from negative to positive occurs at lower Ur for lower Re. This can be seen clearly for two tubes normal to flow, Fig. 5 and triangular array, Fig. 12a; it is also valid for two tubes in tandem, tube row, and square arrays.

Several specific examples can be considered: two tubes in tandem, tube row, triangular array, and square arrays. The stability boundaries for fluid-damping-controlled instability are given in Figs. 19 to 23 as a function of mass-damping parameter, δ_s. Some general features are noted from these figures.

Two Tubes in Tandem (Fig. 19): Fluid-damping-controlled instability occurs at lower δ_s . The lower boundaries vary with P/D but change slowly with δ_s. When P/D is smaller, the critical flow velocity is also lower.

Tube Row (Fig. 20): The general behavior is similar to that of two tubes in tandem. Fluid-damping-controlled instability occurs at lower δ_s. The lowest critical flow velocity increases with tube T/D.

Triangular Array (Fig. 21): Fluid-damping-controlled instability occurs at δ_s less than about 2. It is noted that the instability region depends on Reynolds number. As Reynolds number increases, the region moves upward; this means

that the critical flow velocity is higher. In this case, the size of the instability region is almost independent of Reynolds number.

Square Arrays (Figs. 22 and 23): For square arrays, fluid-damping-controlled instability can occur for various δ_s depending on the location of the tube. Except for the downstream tube, which is similar to triangular array, fluid-damping-controlled instability can occur in the whole range of δ_s. For a tube in the second and third rows, there is a sudden jump of the critical flow velocity at a specific δ_s, $\approx$0.75 and 0.18 for tubes in the second and third rows respectively.

6. CLOSING REMARKS

The unsteady flow theory has been used extensively in the aerospace industry and in bridge flutter. In this paper, a direct-measurement technique for fluid damping and fluid stiffness provides adequate characterization of the fluid effects for fluid-damping-controlled instability for different tube arrays. The critical components of fluid forces are described by α' and β'. Once these two fluid-force coefficients are measured, they can be used in practical applications. Similar data have been used successfully to predict lock-in resonance of a single tube in crossflow (Chen et al. 1995).

A change in response frequency is determined by fluid stiffness and mass ratio, whereas the stability depends on fluid damping. Fluid damping may be negative when α' or β' are positive in some regions; this means that the energy of the fluid is being pumped into the structural system. Based on the sign of α' and β', fluid-damping controlled instability of a single flexible tube in a tube array can be determine immediately.

α' and β' depend on many system parameters: Reynolds number, tube pitch, tube pattern, reduced flow velocity, and oscillation amplitude. Based on the fluid-force coefficients, α' and β', presented in this papers, some general conclusions can be made:

- Fluid-damping-controlled instability is most likely to be associated with the motion in the lift direction since in many cases α' is positive while β' is negative.

- When the reduced flow velocity is small, say $Ur < 10$, α' and β' depend on Reynolds number. At large Ur, Reynolds number has little effect on α' and β'. In the region of Ur in which α' is positive, the crossing point of α' changing from negative to positive or positive to negative shifts to larger Ur as Re increases.

- α' and β' may depend on the pitch-to-diameter ratio. For square arrays, the effect of P/D is very small. This means that for square tube arrays with different P/D, the critical flow velocities for damping-controlled-instability are approximately the same and a single stability criterion can be used for different P/D. On the other hand, for tube rows and triangular arrays, different criteria have to be used for different P/D.

- In the square tube arrays, the most unstable position is the upstream tube and the most stable one is the downstream tube. On the other hand in the triangular tube array, the upstream tube and the tube in the middle of tube array are stable.

- The stability of the downstream tube in various tube arrays is very similar to that of a single tube. This is attributed to the vortex shedding

associated with downstream tube. In all cases, there is a limited range of Ur in which the tube is subjected to fluid-damping-controlled instability.

- For fluid-damping-controlled instability, the interaction effect associated with the motion of the surrounding tubes is less significant. This means that the critical flow velocity of a single flexible tube and that of a group of flexible tube are not very much different. On the other hand, the interaction of multiple tube motions is a necessary condition for fluid-stiffness-controlled instability.

On the basis of the unsteady flow theory, the definition of fluidelastic instability can be defined specifically. Due to fluid damping, when the resultant modal damping ratio becomes zero, the tube is subjected to fluidelastic instability regardless the source of fluid damping. On the other hand, when the modal damping ratio is larger than zero and the tube has large oscillation amplitudes due to other excitation sources such as vortex shedding, this will belong to forced excitation. For example, lock-in resonance due to vortex shedding may be in the fluidelastic instability region or forced excitation depending on Ur and other parameters.

In summary, based on the results, the unsteady flow theory is a simple model that can be used to predict tube response. In addition, the theory points out the role of fluidelastic instability associated with other excitation mechanisms. For example, vortex-induced vibration is a coupled forced vibration and fluidelastic instability when the vortex-shedding frequency is close to the natural frequency of a cylinder. The unsteady flow theory can be used to examine the detailed characteristics in the instability regions as well as forced response due to other excitation sources.

ACKNOWLEDGMENT

This work was funded by Electric Power Research Institute under an agreement with the U.S. Department of Energy, Contract Agreement 31-109-Eng-38-85989.

REFERENCES

Chen, S. S., 1984, "Guidelines for the Instability flow Velocity of Tube Arrays in Crossflow," Journal of Sound and Vibration, Vol. 93, pp. 439-455.

Chen, S. S., 1987a, *Flow-Induced Vibration of Circular Cylindrical Structures*, Hemisphere Publishing Corp., New York, NY.

Chen, S. S. 1987b, "A General Theory for Dynamic Instability of Tube Arrays in Crossflow," Journal of Fluids and Structures, Vol. 1, pp. 35-53.

Chen, S. S., and Jendrzejczyk, J. A., 1981, "Experiments on Fluid Elastic Instability in Tube Banks Subjected to Liquid Cross Flow," Journal of Sound and Vibration, Vol. 78(3), pp. 355-381.

Chen, S. S., Cai, Y., and Zhu, S., 1996, "Flow-Induced Vibration of Tubes in Crossflow," Journal of Offshore Mechanics & Arctic Engineering, Vol. 118(4), pp. 253-258.

Chen, S. S., Zhu, S., and Cai, Y., 1995, "An Unsteady Flow Theory for Vortex-Induced Vibration," Journal of Sound and Vibration, Vol. 184(1), pp. 73-92.

Chen, S. S., Zhu, S., and Jendrzejczyk, J. A., 1994, "Fluid Damping and Fluid Stiffness of a Tube Row in Crossflow," Journal of Pressure Vessel Technology, Vol. 116, pp. 370-383.

Chen, S. S. 1983a, "Instability Mechanisms and Stability Criteria of a Group of Circular Cylinders Subjected to Cross Flow: Part I, Theory," Journal of Vibration, Acoustics, Stress and Reliability in Design, Vol. 105, pp. 51-58.

Chen, S. S. 1983b, "Instability Mechanisms and Stability Criteria of a Group of Circular Cylinders Subjected to Cross Flow: Part II, Numerical Results and Discussions," Journal of Vibration, Acoustics, Stress and Reliability in Design, Vol. 105, pp. 253-260.

Connors, H. J., 1970, "Fluidelastic Vibration of Tube Arrays Excited by Cross Flow," *Flow-Induced Vibration in Heat Exchangers*, ed., D. D. Reiff, ASME, New York, NY, pp. 42-56.

Price, S. J., 1993, "Theoretical Models of Fluidelastic Instability for Cylinder Arrays Subjected to Cross Flow," *Technology for the '90s, A Decade of Progress*, The ASME Pressure Vessels and Piping Division, pp. 711-773.

Price, S. J., Mark, B., and Paidoussis, M. P., 1986, "An Experimental Stability Analysis of a Single Flexible Cylinder Positioned in an Array of Rigid Cylinders and Subject to Cross-Flow," Journal of Pressure Vessel Technology, Vol. 108, pp. 62-72.

Price, S. J., and Paidoussis, M. P., 1987, "The Flow-Induced Response of a Single Flexible Cylinder in an In-Line Array of Rigid Cylinders," Proc. Intl. Conf. Flow-Induced Vibrations, Bowness-on-Windermere, UK, Paper B1, pp. 51-63.

Tanaka, H., 1980, "Study on Fluidelastic Vibration of Tube Bundle," Nihon Kikai Gakkai Ronbunshu, or Japan Society of Mechanical Engineering, Section B, Vol. 46, pp. 1398-1407.

Tanaka, H., and Takahara, S., 1981, "Fluid Elastic Vibration of Tube Array in Cross Flow," Journal of Sound and Vibration, Vol. 77, pp. 19-37.

Tanaka, H., Takahara, S., and Ohta, K., 1982, "Flow-Induced Vibration of Tube Arrays with Various Pitch-to-Diameter Ratios," ASME Journal of Pressure Vessel Technology, Vol. 104, pp. 168-174.

Zhu, S., Cai, Y., and Chen, S. S., 1995, "Experimental Fluid-Force Coefficients for Wake-Induced Cylinder Vibration," Journal of Engineering Mechanics, Vol. 121, pp. 1003-1005.

Zhu, S., Chen, S. S., and Cai, Y., 1996, "Vibration and Stability of Two Tubes in Crossflow," To appear in Journal of Pressure Vessel Technology.

Figure Captions

1 Tube oscillating in crossflow.

2 Tube arrays in crossflow: (a) single tube; (b) two tubes normal to flow; (c) two tubes in tandem; (d) a tube in the wake of another tube; (e) tube row; (f) triangular array; and (g, h, i) square arrays.

3 Fluid-stiffness coefficient α'' and fluid-damping coefficient α' for a single tube (Case a) for three Reynolds numbers.

4 Fluid-stiffness coefficient α'' and fluid-damping coefficient α' for a single tube (Case a) for Re = 2760.

5 Fluid-stiffness coefficients α'' and β'' and fluid-damping coefficients α' and β' for two tubes normal to flow (Case b).

6 Fluid-stiffness coefficients α'' and β'' and fluid-damping coefficients α' and β' for the upstream tube of two tubes in tandem (Case c).

7 Fluid-stiffness and fluid-damping coefficient for the downstream tube of two tubes in tandem (Case c): (a) α'' and α'; and (b) β'' and β'.

8 Fluid-stiffness and fluid-damping coefficient for a tube in the wake of another tube (Case d): (a) α'' and α'; and (b) β'' and β'.

9 Fluid-stiffness coefficient α'' and fluid-damping coefficient α' for tube row with T/D = 1.35 (Case e.1) for three Re.

10 Fluid-stiffness coefficient α'' and fluid-damping coefficient α' for tube row with T/D = 1.35 (Case e.1) for Re = 3140.

11 Fluid-stiffness coefficient α'' and fluid-damping coefficient α' for tube row with T/D = 2.7 (Case e.2).

12 Fluid-stiffness and fluid-damping coefficient for triangular array (Case f): (a) α'' and α'; and (b) β'' and β'.

13 Fluid-stiffness and fluid-damping coefficient for square tube array with P/D = 1.35 (Case g): (a) α'; (b) α''; (c) β'; and (d) β''.

14 Fluid-stiffness coefficients α'' and β'' and fluid-damping coefficients α' and β' for square tube array with P/D = 1.42 (Case h).

15 Fluid-stiffness and fluid-damping coefficient for square array with P/D = 1.46 (Case i): (a) α'' and α'; and (b) β'' and β'.

16 Fluid-damping coefficient α' at different locations for square array with P/D = 1.46.

17 Fluid-damping coefficient α' for square array with different P/D.

18 Fluid-damping coefficient α' of the downstream tube for various tube arrays.

19 Fluid-damping-controlled instability boundaries for two tubes in tandem, Cases c.1, c.2, and c.3.

20 Fluid-damping-controlled instability boundaries for tube rows, Cases e.1 and e.2.

21 Fluid-damping-controlled instability boundaries for triangular array, Case f.3.

22 Fluid-damping-controlled instability boundaries for square array, Cases g.1, g.2, g.3, and g.4.

23 Fluid-damping-controlled instability boundaries for square array, Cases g.4 and i.3.

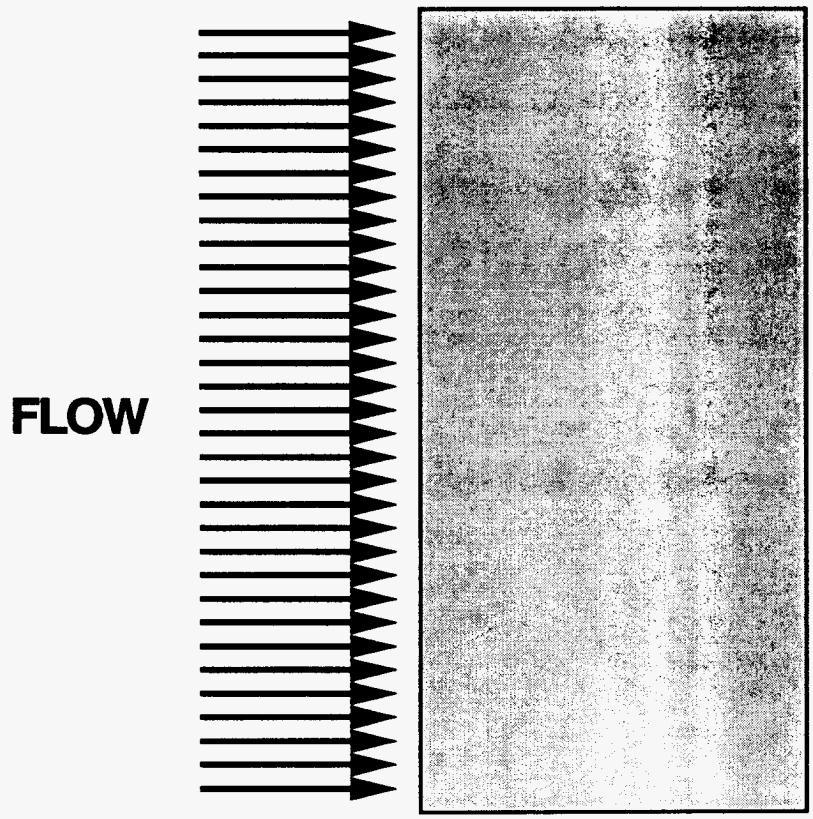

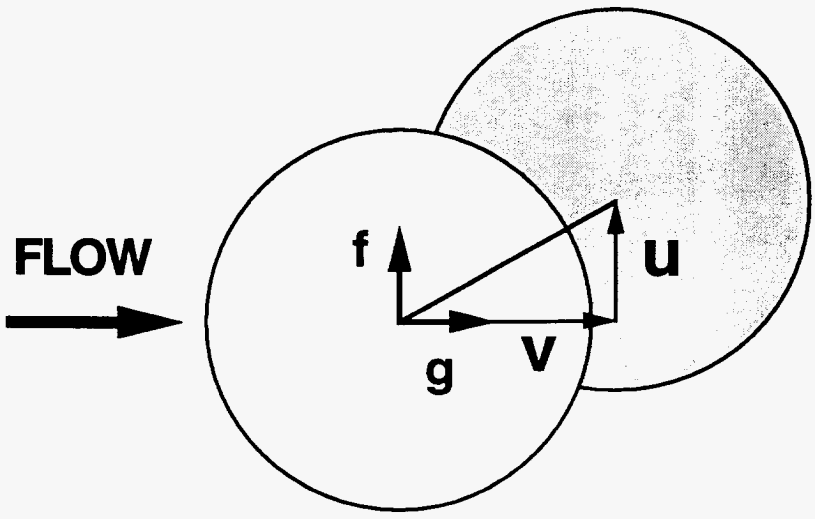

Fig. 1

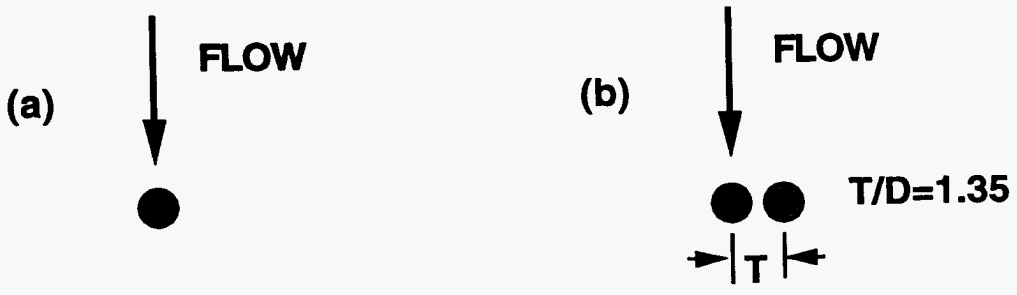

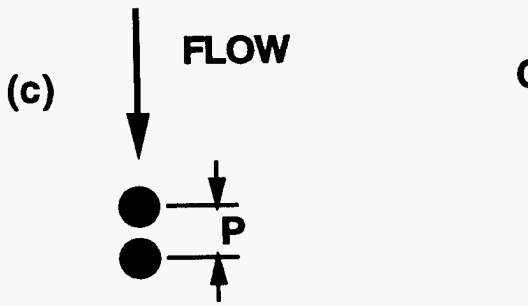

CASE	P/D
c.1	1.35
c.2	2.70
c.3	4.05

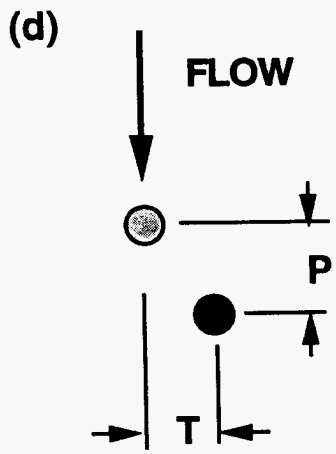

CASE	P/D	T/D
d.1	2.70	1.35
d.2	4.05	1.35
d.3	4.05	2.70

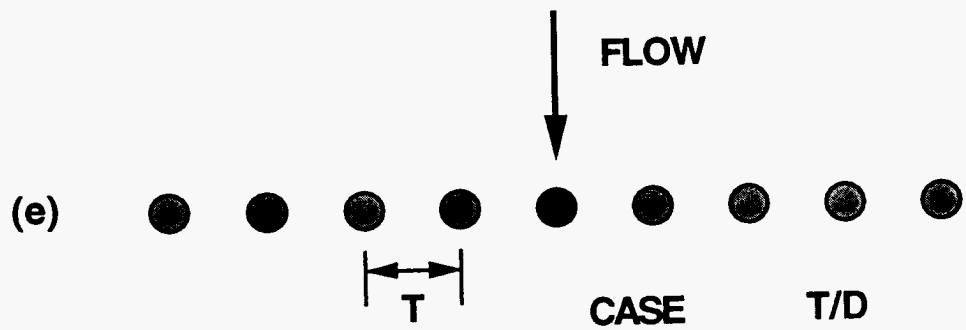

CASE	T/D
e.1	1.35
e.2	2.70

Fig. 2.1

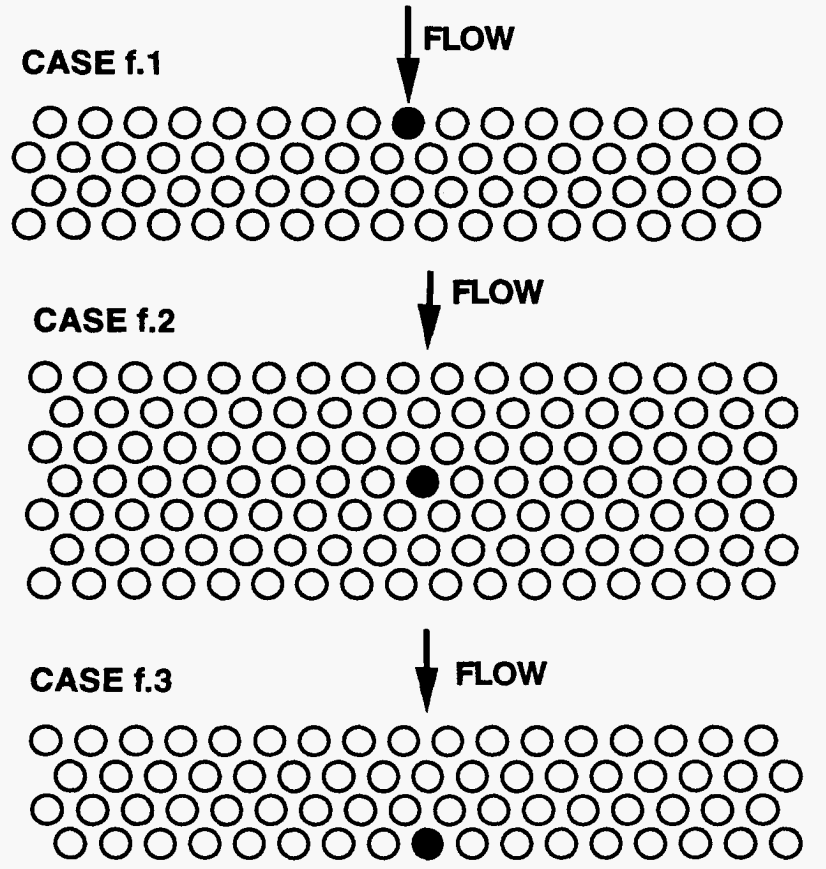

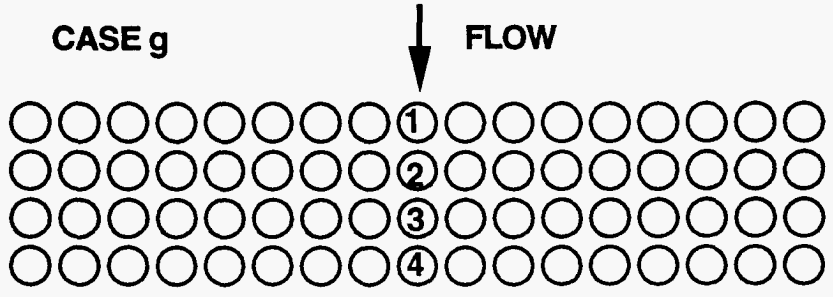

Fig. 2.2

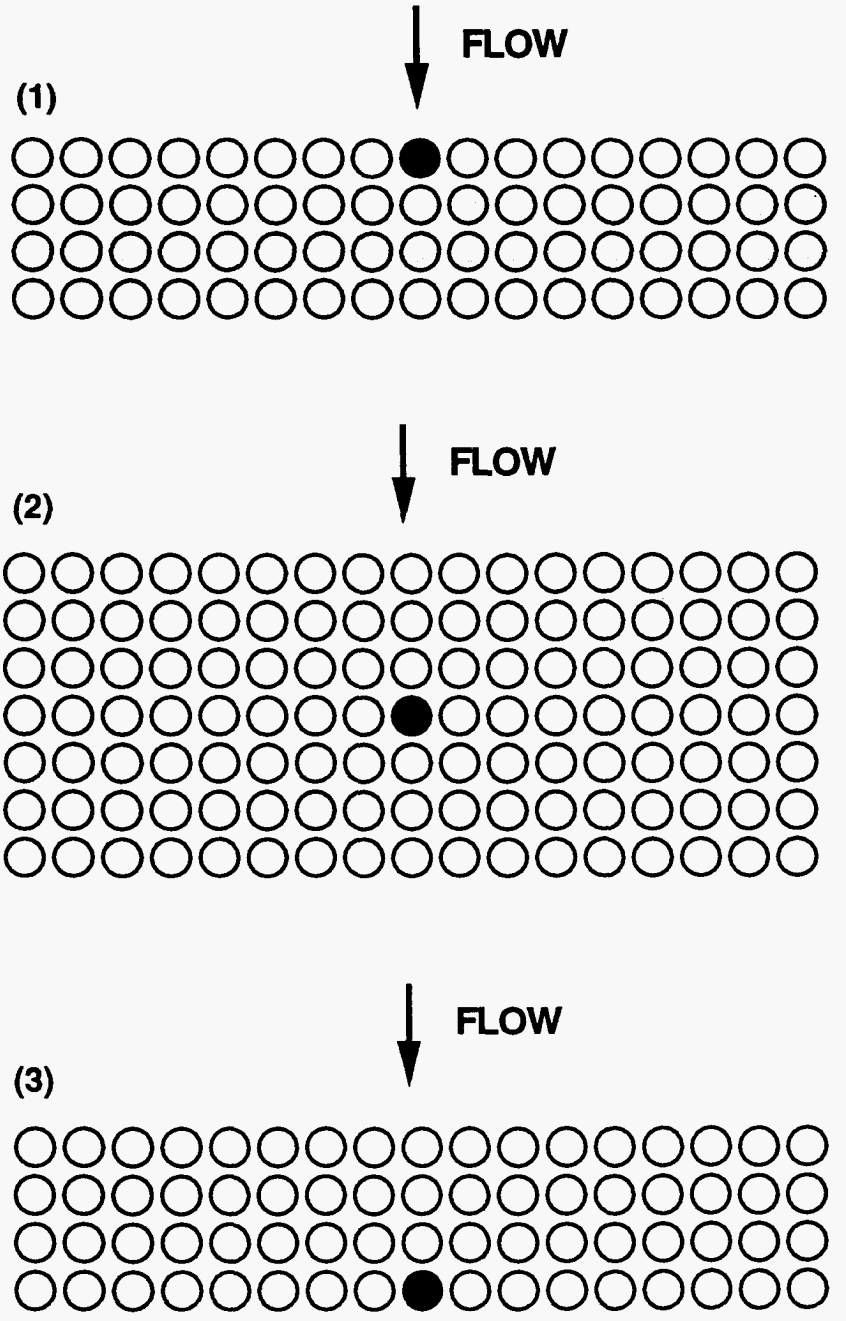

CASE	P/D	T/D
h	1.42	1.42
i	1.46	1.46

Fig. 2.3

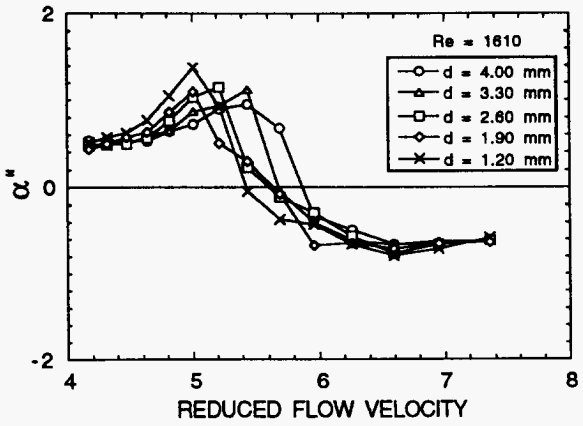
Re = 1610
d = 4.00 mm
d = 3.30 mm
d = 2.60 mm
d = 1.90 mm
d = 1.20 mm
α"
REDUCED FLOW VELOCITY

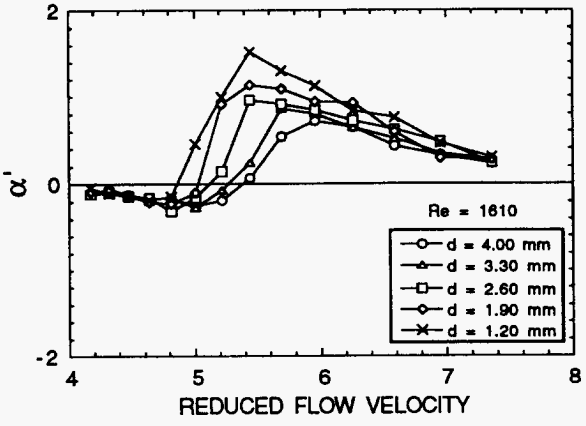
Re = 1610
d = 4.00 mm
d = 3.30 mm
d = 2.60 mm
d = 1.90 mm
d = 1.20 mm
α'
REDUCED FLOW VELOCITY

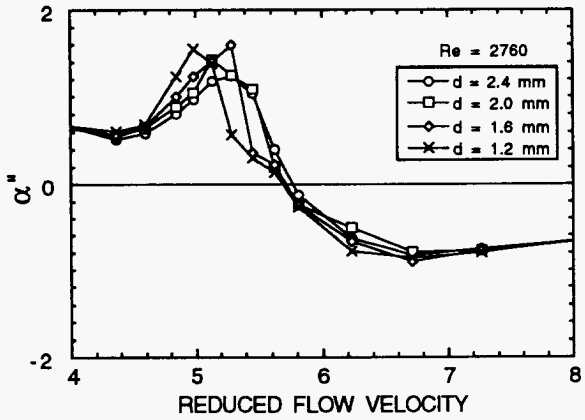
Re = 2760
d = 2.4 mm
d = 2.0 mm
d = 1.6 mm
d = 1.2 mm
α"
REDUCED FLOW VELOCITY

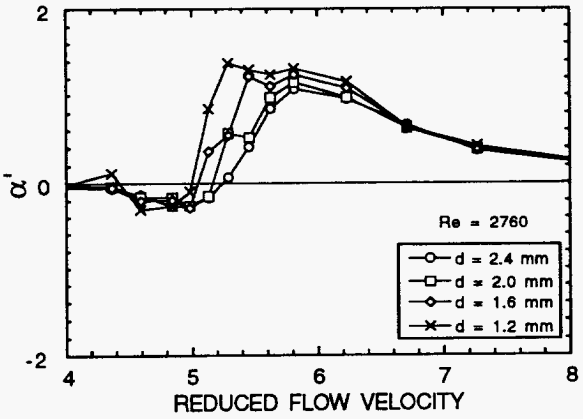
Re = 2760
d = 2.4 mm
d = 2.0 mm
d = 1.6 mm
d = 1.2 mm
α'
REDUCED FLOW VELOCITY

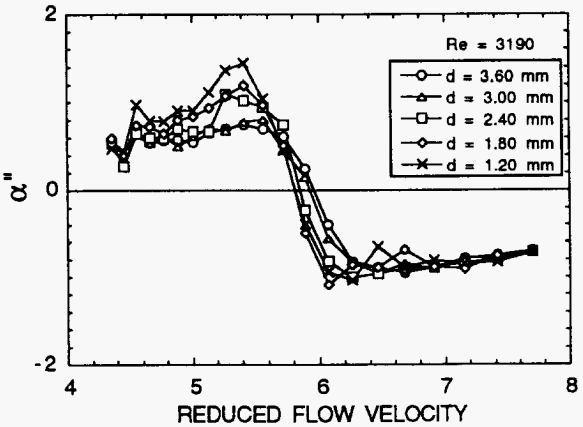
Re = 3190
d = 3.60 mm
d = 3.00 mm
d = 2.40 mm
d = 1.80 mm
d = 1.20 mm
α"
REDUCED FLOW VELOCITY

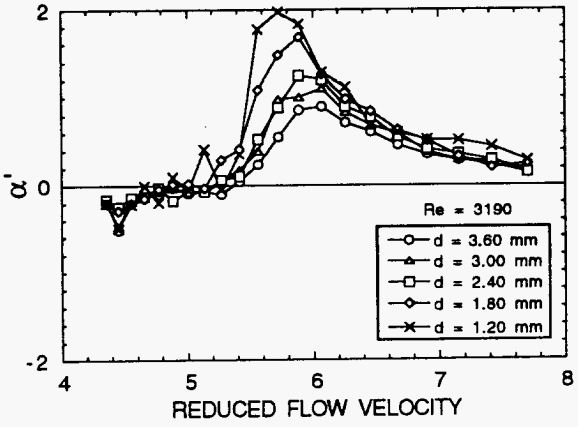
Re = 3190
d = 3.60 mm
d = 3.00 mm
d = 2.40 mm
d = 1.80 mm
d = 1.20 mm
α'
REDUCED FLOW VELOCITY

Fig 3

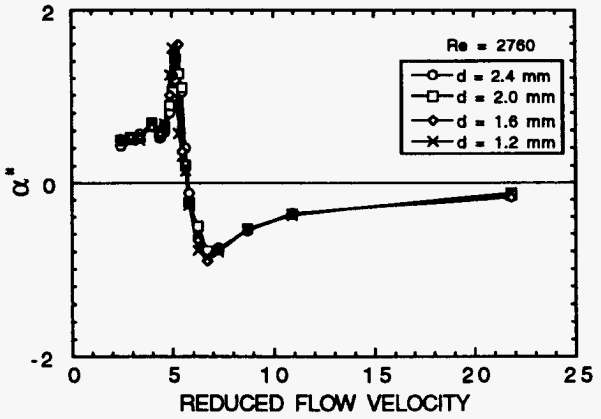
Re = 2760
d = 2.4 mm
d = 2.0 mm
d = 1.6 mm
d = 1.2 mm
α"
2
0
-2
0
5
10
15
20
25
REDUCED FLOW VELOCITY

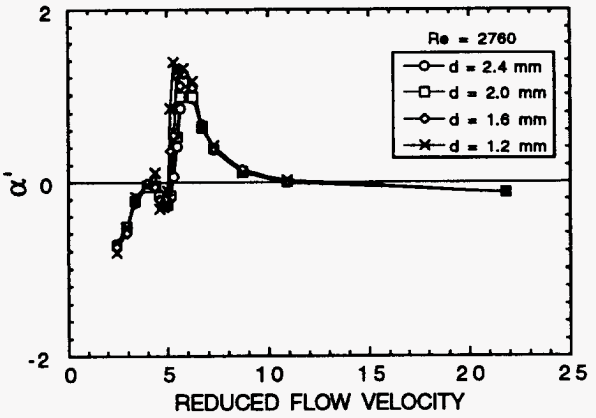
Re = 2760
d = 2.4 mm
d = 2.0 mm
d = 1.6 mm
d = 1.2 mm
α'
2
0
-2
0
5
10
15
20
25
REDUCED FLOW VELOCITY

Fig. 4

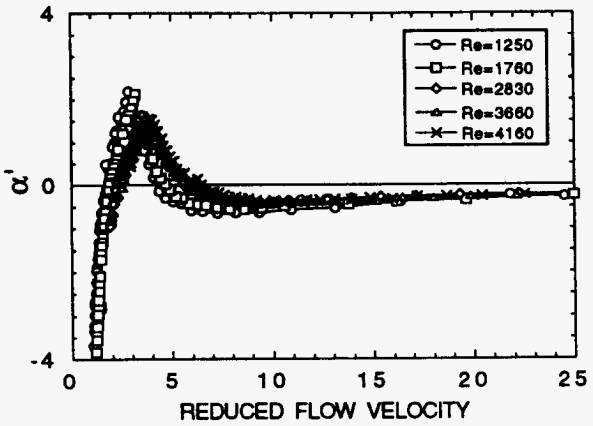
Re=1250
Re=1760
Re=2830
Re=3660
Re=4160
α'
4
0
-4
0
5
10
15
20
25
REDUCED FLOW VELOCITY

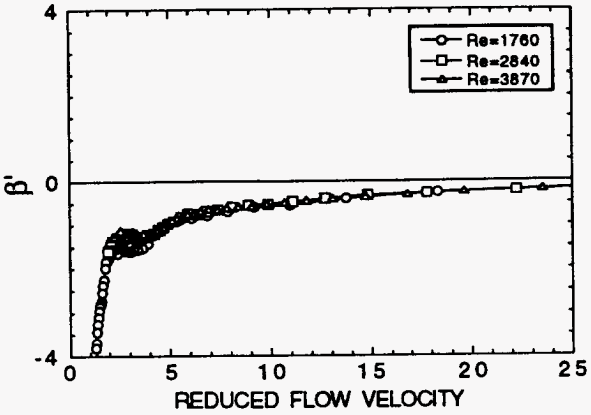
Re=1760
Re=2840
Re=3870
β'
4
0
-4
0
5
10
15
20
25
REDUCED FLOW VELOCITY

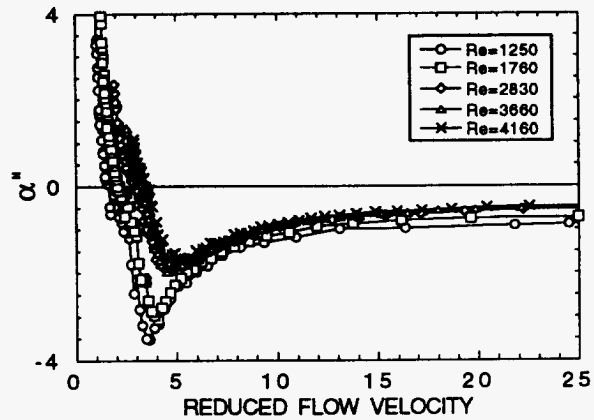
Re=1250
Re=1760
Re=2830
Re=3660
Re=4160
α"
4
0
-4
0
5
10
15
20
25
REDUCED FLOW VELOCITY

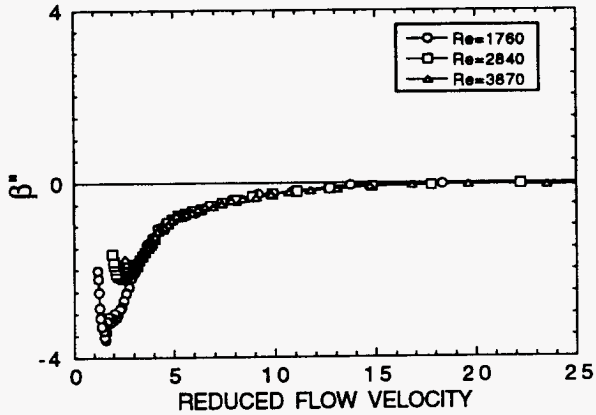
Re=1760
Re=2840
Re=3870
β"
4
0
-4
0
5
10
15
20
25
REDUCED FLOW VELOCITY

Fig. 5

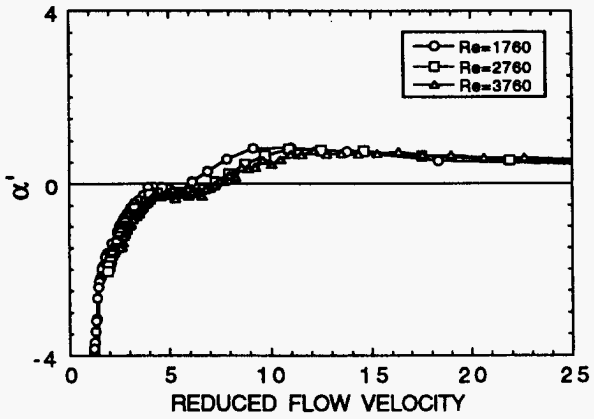
Re=1760
Re=2760
Re=3760
α'
4
0
-4
0
5
10
15
20
25
REDUCED FLOW VELOCITY

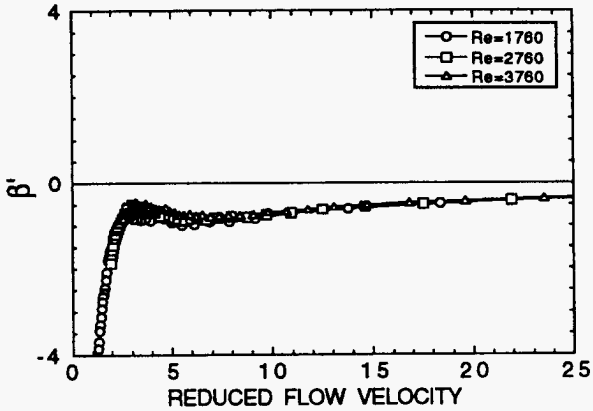
Re=1760
Re=2760
Re=3760
β'
4
0
-4
0
5
10
15
20
25
REDUCED FLOW VELOCITY

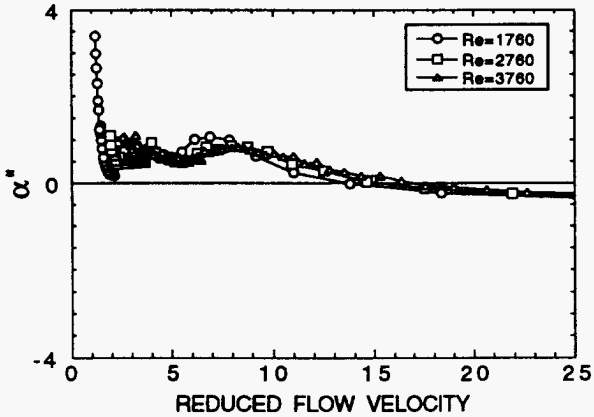
Re=1760
Re=2760
Re=3760
α"
4
0
-4
0
5
10
15
20
25
REDUCED FLOW VELOCITY

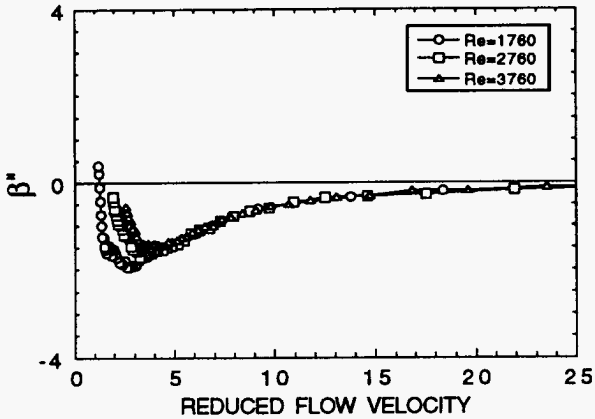
Re=1760
Re=2760
Re=3760
β"
4
0
-4
0
5
10
15
20
25
REDUCED FLOW VELOCITY

Fig. 6

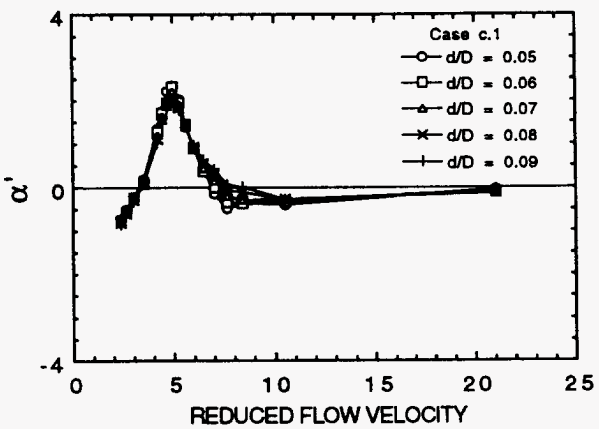
Case c.1
d/D = 0.05
d/D = 0.06
d/D = 0.07
d/D = 0.08
d/D = 0.09
α'
4
0
-4
0
5
10
15
20
25
REDUCED FLOW VELOCITY

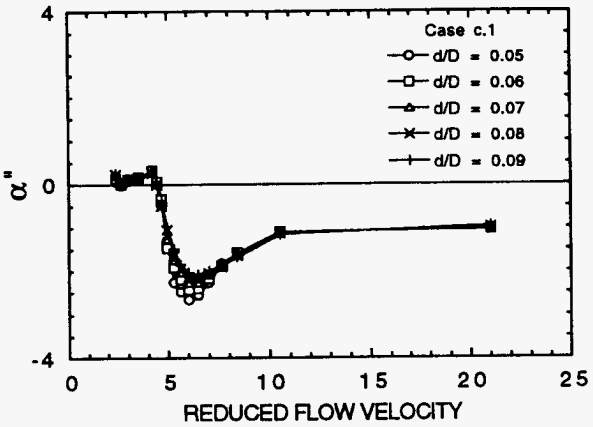
Case c.1
d/D = 0.05
d/D = 0.06
d/D = 0.07
d/D = 0.08
d/D = 0.09
α"
4
0
-4
0
5
10
15
20
25
REDUCED FLOW VELOCITY

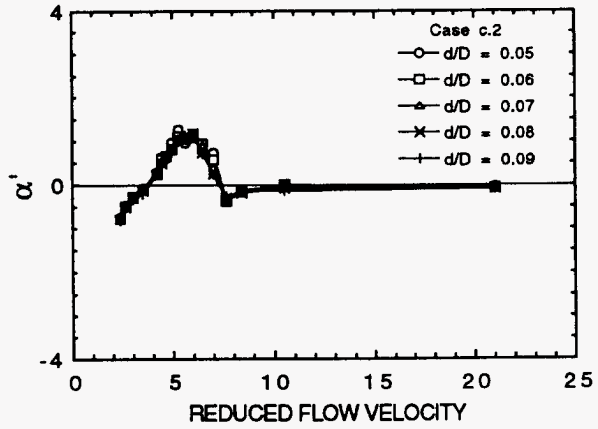
Case c.2
d/D = 0.05
d/D = 0.06
d/D = 0.07
d/D = 0.08
d/D = 0.09
α'
4
0
-4
0
5
10
15
20
25
REDUCED FLOW VELOCITY

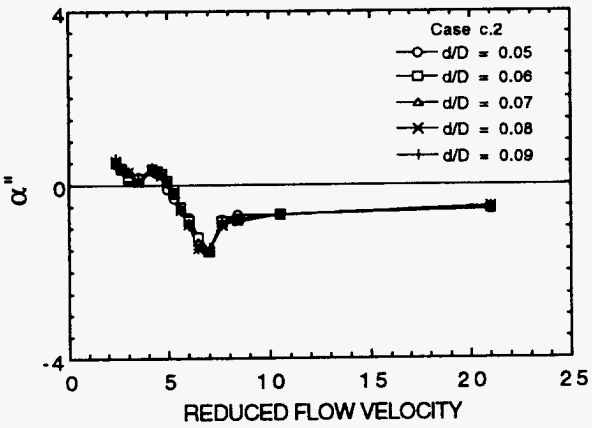
Case c.2
d/D = 0.05
d/D = 0.06
d/D = 0.07
d/D = 0.08
d/D = 0.09
α"
4
0
-4
0
5
10
15
20
25
REDUCED FLOW VELOCITY

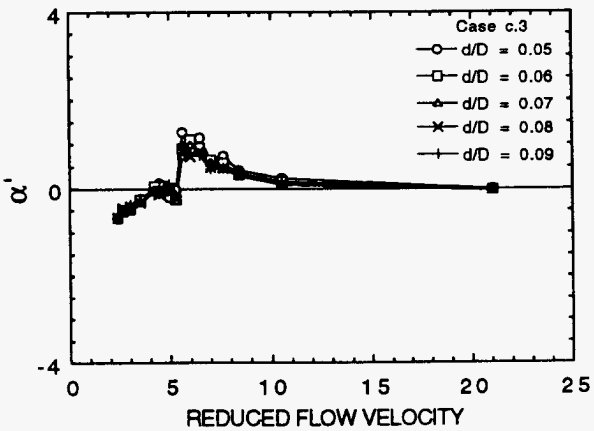
Case c.3
d/D = 0.05
d/D = 0.06
d/D = 0.07
d/D = 0.08
d/D = 0.09
α'
4
0
-4
0
5
10
15
20
25
REDUCED FLOW VELOCITY

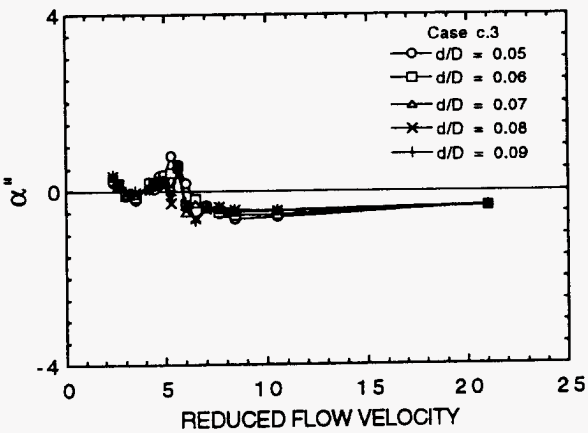
Case c.3
d/D = 0.05
d/D = 0.06
d/D = 0.07
d/D = 0.08
d/D = 0.09
α"
4
0
-4
0
5
10
15
20
25
REDUCED FLOW VELOCITY

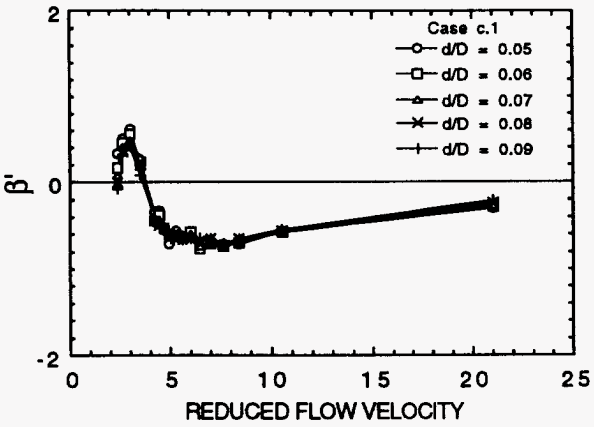
Case c.1
d/D = 0.05
d/D = 0.06
d/D = 0.07
d/D = 0.08
d/D = 0.09
β'
REDUCED FLOW VELOCITY

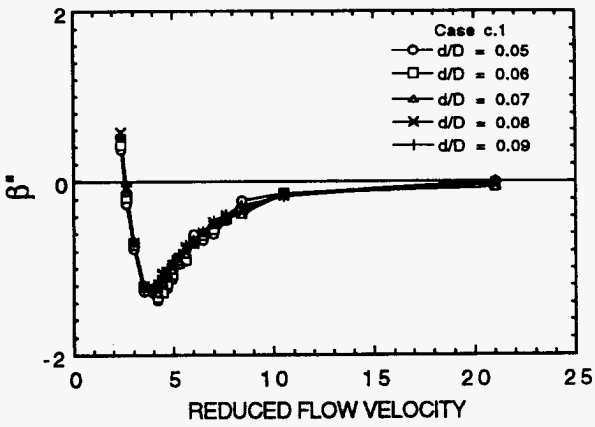
Case c.1
d/D = 0.05
d/D = 0.06
d/D = 0.07
d/D = 0.08
d/D = 0.09
β"
REDUCED FLOW VELOCITY

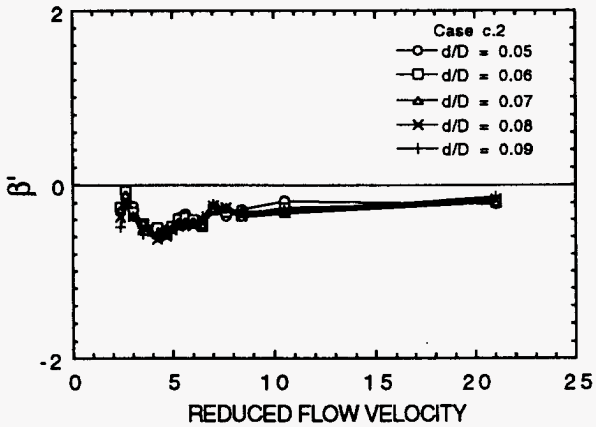
Case c.2
d/D = 0.05
d/D = 0.06
d/D = 0.07
d/D = 0.08
d/D = 0.09
β'
REDUCED FLOW VELOCITY

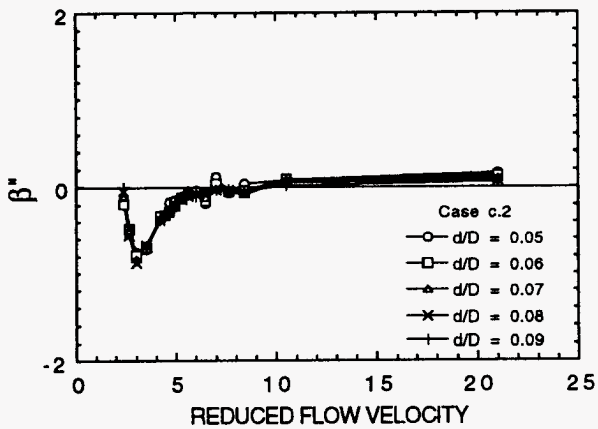
Case c.2
d/D = 0.05
d/D = 0.06
d/D = 0.07
d/D = 0.08
d/D = 0.09
β"
REDUCED FLOW VELOCITY

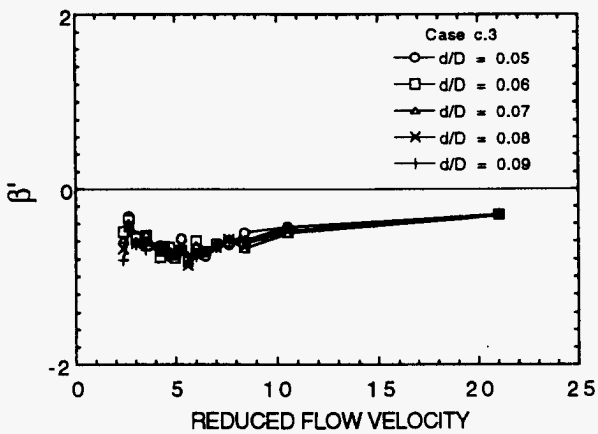
Case c.3
d/D = 0.05
d/D = 0.06
d/D = 0.07
d/D = 0.08
d/D = 0.09
β'
REDUCED FLOW VELOCITY

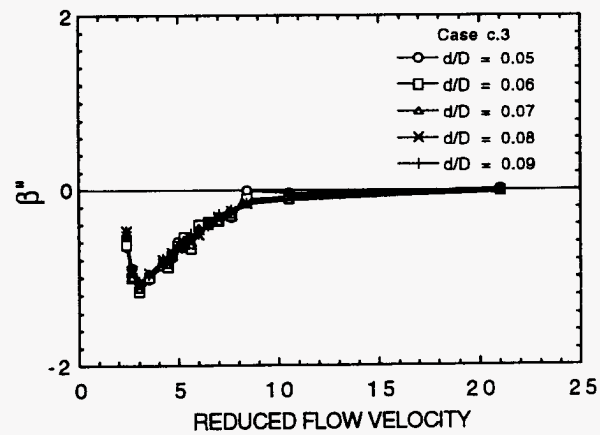
Case c.3
d/D = 0.05
d/D = 0.06
d/D = 0.07
d/D = 0.08
d/D = 0.09
β"
REDUCED FLOW VELOCITY

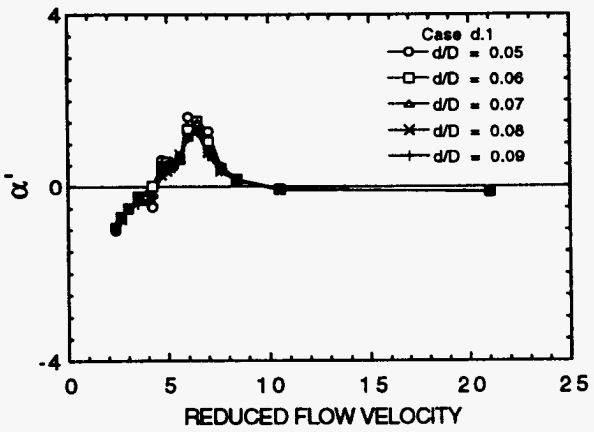
Case d.1
d/D = 0.05
d/D = 0.06
d/D = 0.07
d/D = 0.08
d/D = 0.09
α'
REDUCED FLOW VELOCITY

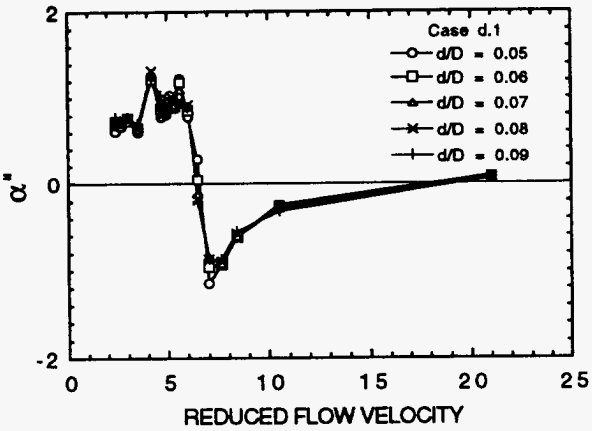
Case d.1
d/D = 0.05
d/D = 0.06
d/D = 0.07
d/D = 0.08
d/D = 0.09
α"
REDUCED FLOW VELOCITY

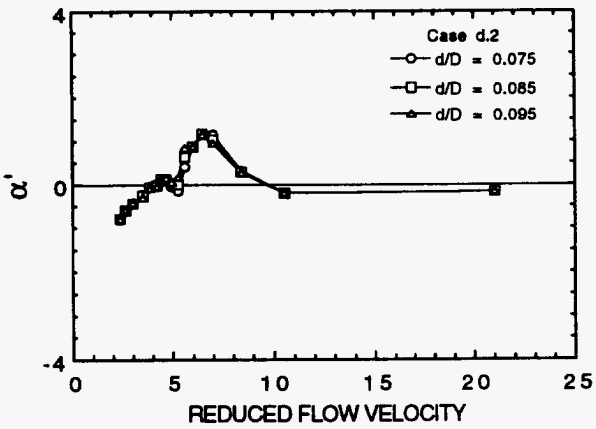
Case d.2
d/D = 0.075
d/D = 0.085
d/D = 0.095
α'
REDUCED FLOW VELOCITY

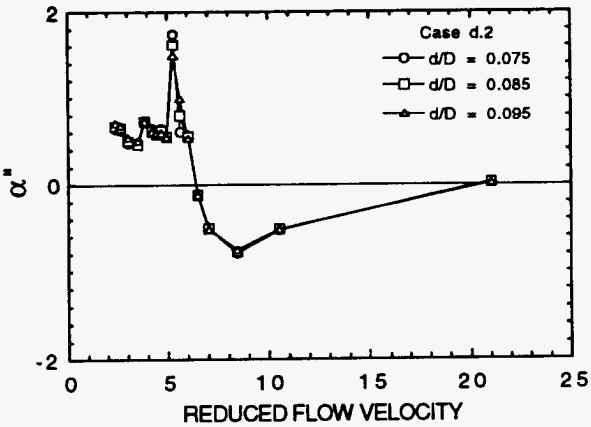
Case d.2
d/D = 0.075
d/D = 0.085
d/D = 0.095
α"
REDUCED FLOW VELOCITY

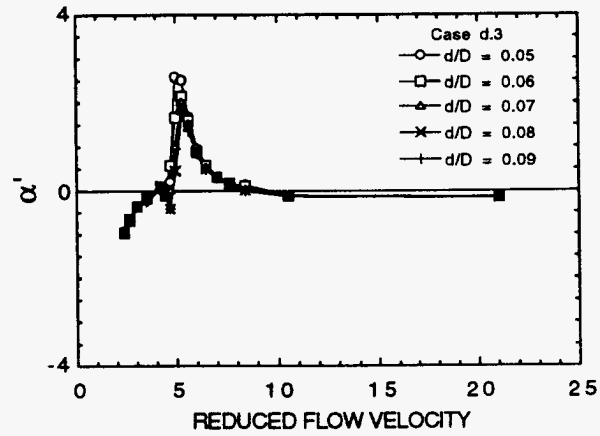
Case d.3
d/D = 0.05
d/D = 0.06
d/D = 0.07
d/D = 0.08
d/D = 0.09
α'
REDUCED FLOW VELOCITY

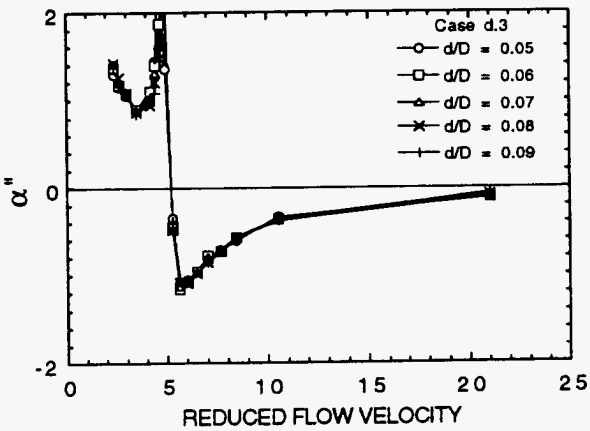
Case d.3
d/D = 0.05
d/D = 0.06
d/D = 0.07
d/D = 0.08
d/D = 0.09
α"
REDUCED FLOW VELOCITY

Fig. 8a

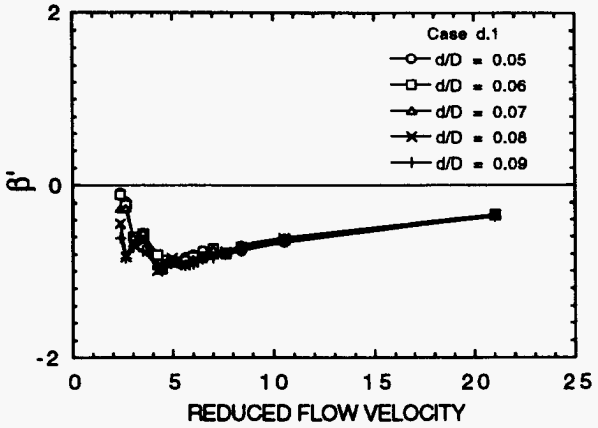
Case d.1
d/D = 0.05
d/D = 0.06
d/D = 0.07
d/D = 0.08
d/D = 0.09
β'
2
0
-2
0
5
10
15
20
25
REDUCED FLOW VELOCITY

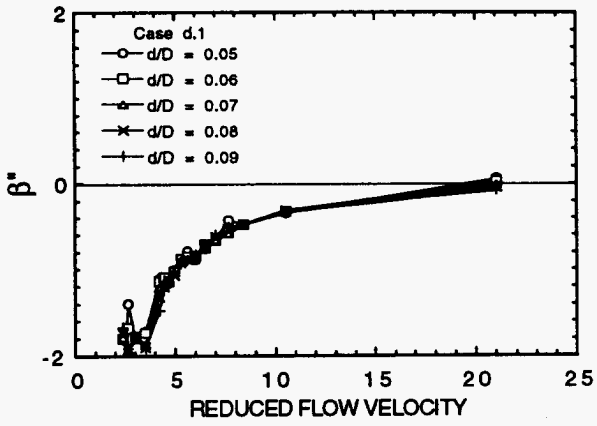
Case d.1
d/D = 0.05
d/D = 0.06
d/D = 0.07
d/D = 0.08
d/D = 0.09
β"
2
0
-2
0
5
10
15
20
25
REDUCED FLOW VELOCITY

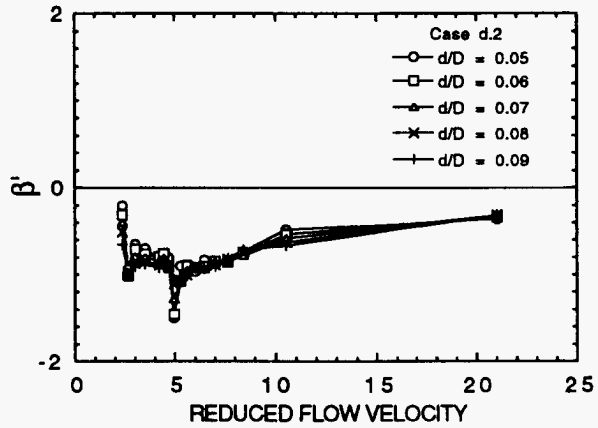
Case d.2
d/D = 0.05
d/D = 0.06
d/D = 0.07
d/D = 0.08
d/D = 0.09
β'
2
0
-2
0
5
10
15
20
25
REDUCED FLOW VELOCITY

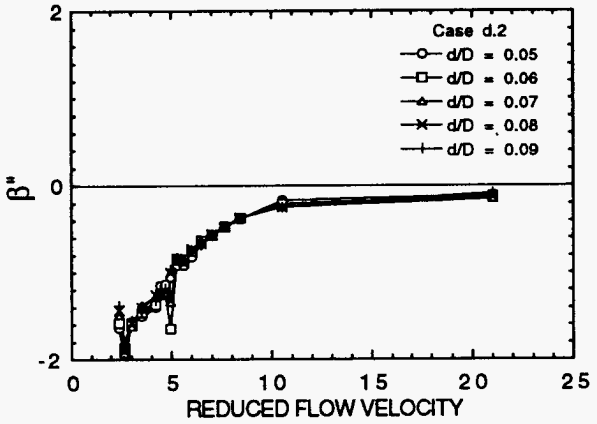
Case d.2
d/D = 0.05
d/D = 0.06
d/D = 0.07
d/D = 0.08
d/D = 0.09
β"
2
0
-2
0
5
10
15
20
25
REDUCED FLOW VELOCITY

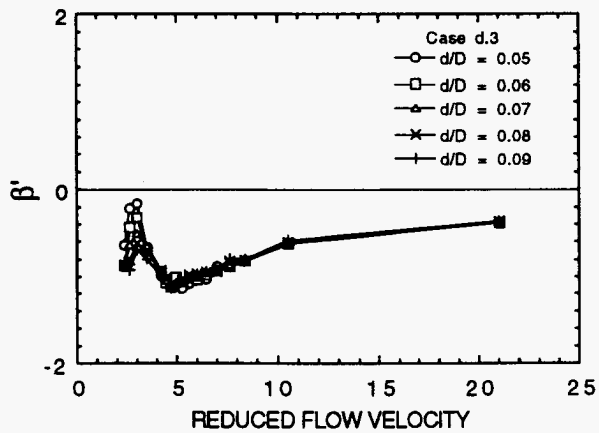
Case d.3
d/D = 0.05
d/D = 0.06
d/D = 0.07
d/D = 0.08
d/D = 0.09
β'
2
0
-2
0
5
10
15
20
25
REDUCED FLOW VELOCITY

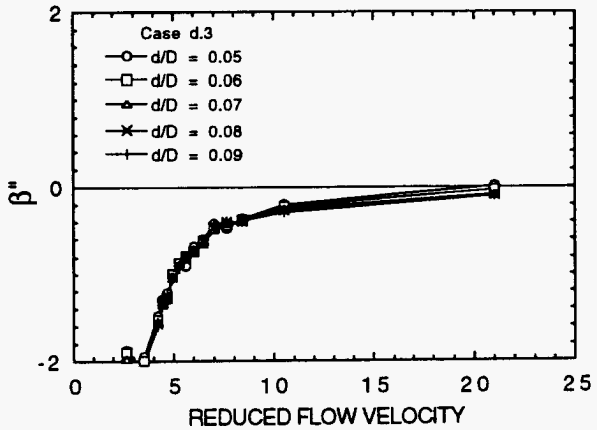
Case d.3
d/D = 0.05
d/D = 0.06
d/D = 0.07
d/D = 0.08
d/D = 0.09
β"
2
0
-2
0
5
10
15
20
25
REDUCED FLOW VELOCITY

Fig. 8a

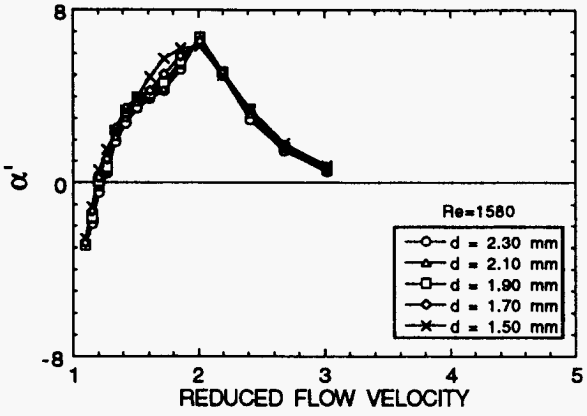
α'
8
0
-8
1
2
3
4
5
REDUCED FLOW VELOCITY
Re=1580
d = 2.30 mm
d = 2.10 mm
d = 1.90 mm
d = 1.70 mm
d = 1.50 mm

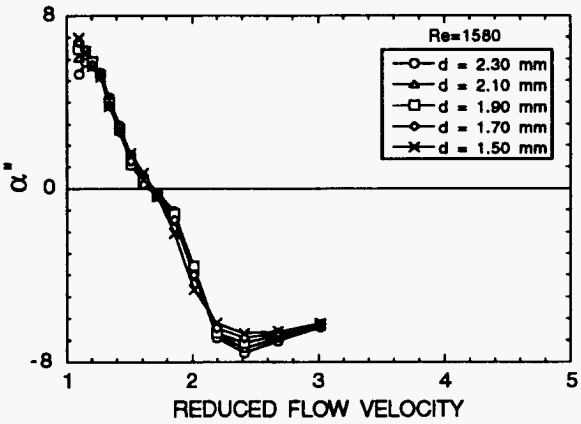
α"
8
0
-8
1
2
3
4
5
REDUCED FLOW VELOCITY
Re=1580
d = 2.30 mm
d = 2.10 mm
d = 1.90 mm
d = 1.70 mm
d = 1.50 mm

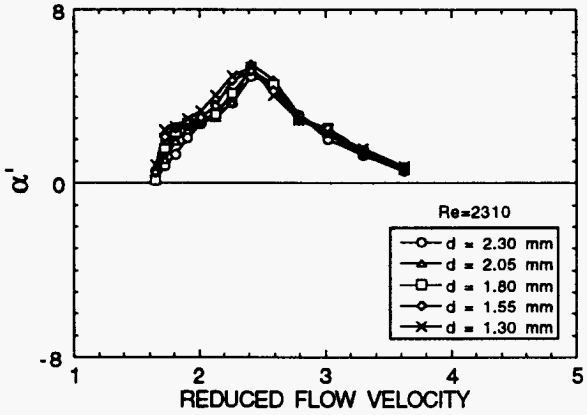
α'
8
0
-8
1
2
3
4
5
REDUCED FLOW VELOCITY
Re=2310
d = 2.30 mm
d = 2.05 mm
d = 1.80 mm
d = 1.55 mm
d = 1.30 mm

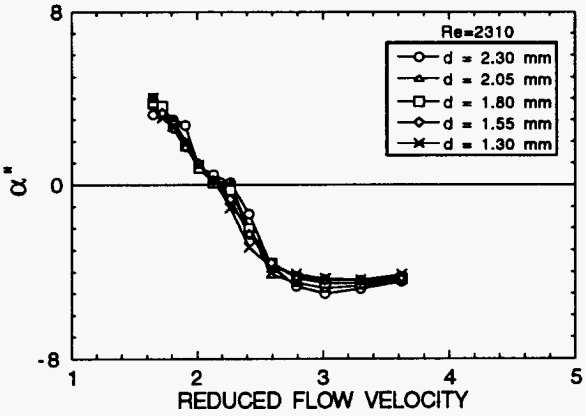
α"
8
0
-8
1
2
3
4
5
REDUCED FLOW VELOCITY
Re=2310
d = 2.30 mm
d = 2.05 mm
d = 1.80 mm
d = 1.55 mm
d = 1.30 mm

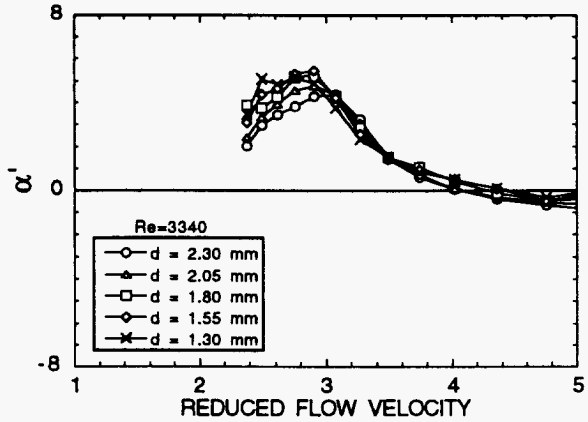
α'
8
0
-8
1
2
3
4
5
REDUCED FLOW VELOCITY
Re=3340
d = 2.30 mm
d = 2.05 mm
d = 1.80 mm
d = 1.55 mm
d = 1.30 mm

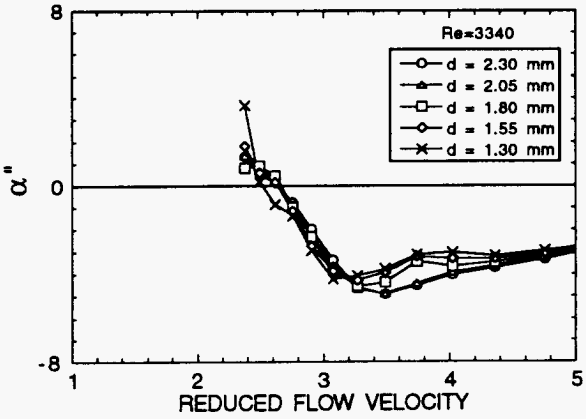
α"
8
0
-8
1
2
3
4
5
REDUCED FLOW VELOCITY
Re=3340
d = 2.30 mm
d = 2.05 mm
d = 1.80 mm
d = 1.55 mm
d = 1.30 mm

Fig. 9

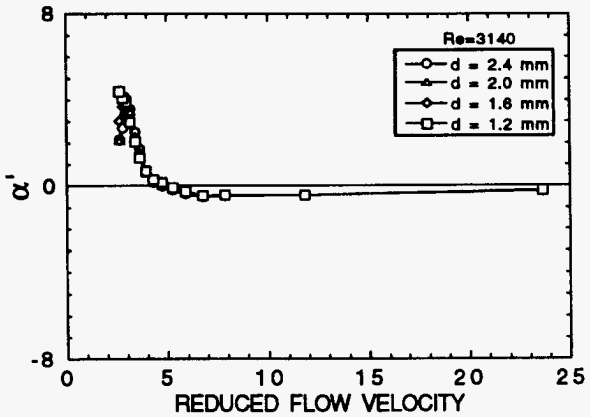
Re=3140
d = 2.4 mm
d = 2.0 mm
d = 1.6 mm
d = 1.2 mm
α'
8
0
-8
0
5
10
15
20
25
REDUCED FLOW VELOCITY

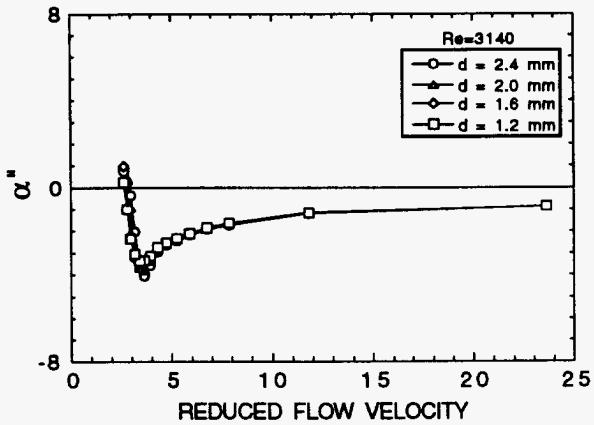
Re=3140
d = 2.4 mm
d = 2.0 mm
d = 1.6 mm
d = 1.2 mm
α"
8
0
-8
0
5
10
15
20
25
REDUCED FLOW VELOCITY

Fig. 3

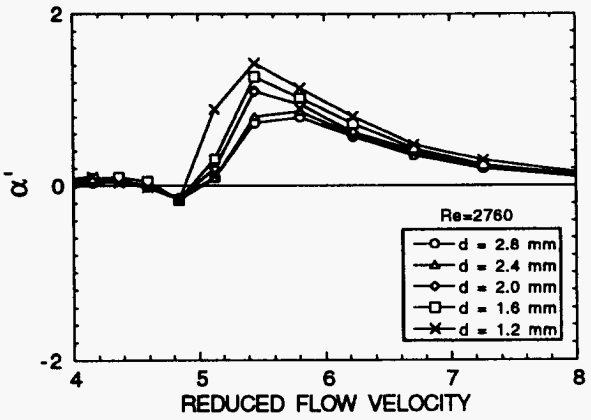
α'
Re=2760
d = 2.8 mm
d = 2.4 mm
d = 2.0 mm
d = 1.6 mm
d = 1.2 mm
REDUCED FLOW VELOCITY

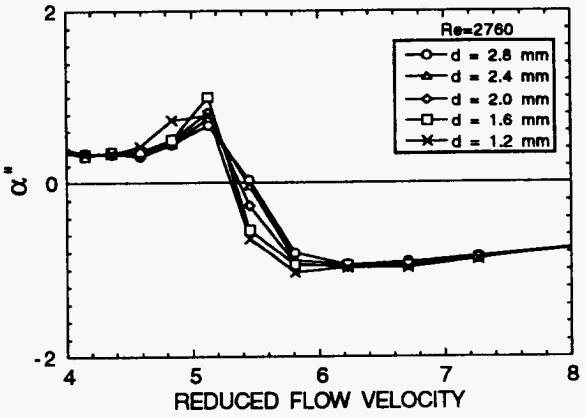
α"
Re=2760
d = 2.8 mm
d = 2.4 mm
d = 2.0 mm
d = 1.6 mm
d = 1.2 mm
REDUCED FLOW VELOCITY

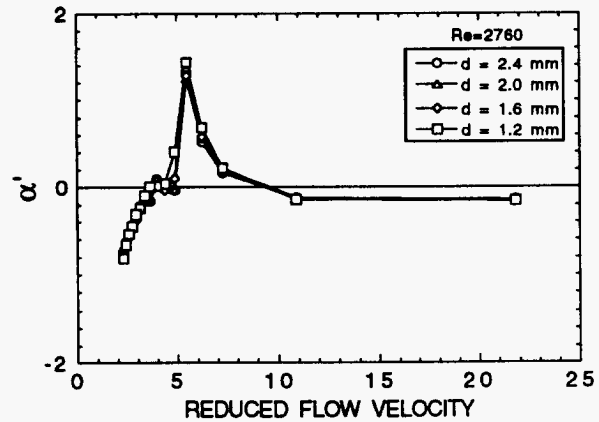
α'
Re=2760
d = 2.4 mm
d = 2.0 mm
d = 1.6 mm
d = 1.2 mm
REDUCED FLOW VELOCITY

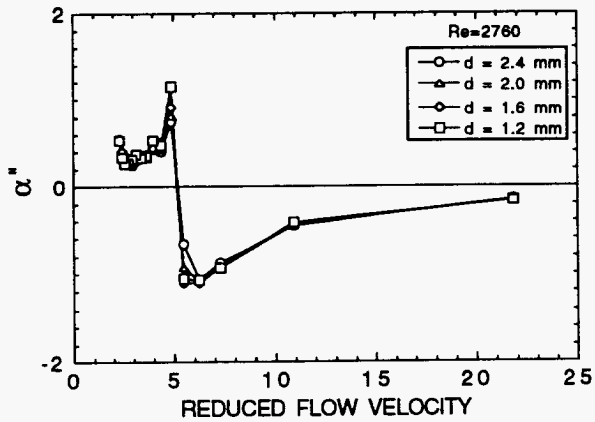
α"
Re=2760
d = 2.4 mm
d = 2.0 mm
d = 1.6 mm
d = 1.2 mm
REDUCED FLOW VELOCITY

Fig. 11

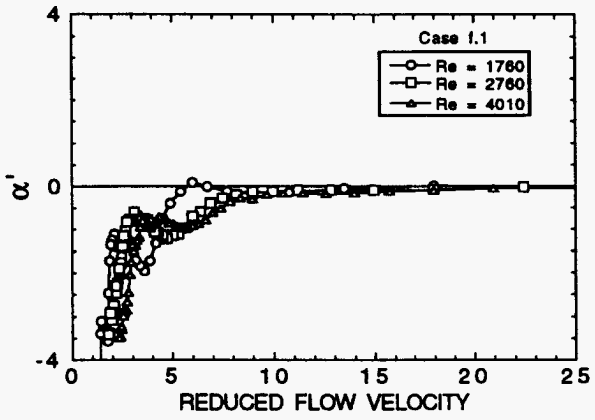
Case f.1
Re = 1760
Re = 2760
Re = 4010
α'
4
0
-4
0
5
10
15
20
25
REDUCED FLOW VELOCITY

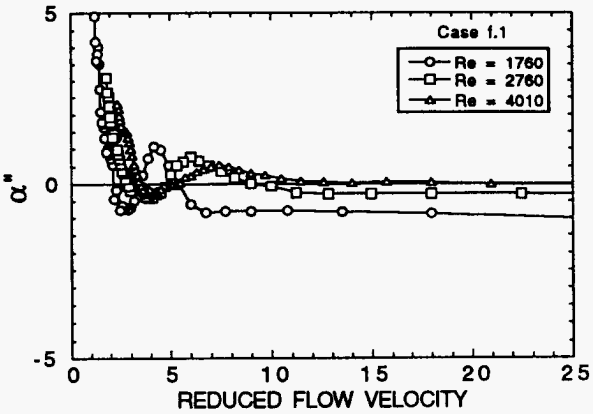
Case f.1
Re = 1760
Re = 2760
Re = 4010
α"
5
0
-5
0
5
10
15
20
25
REDUCED FLOW VELOCITY

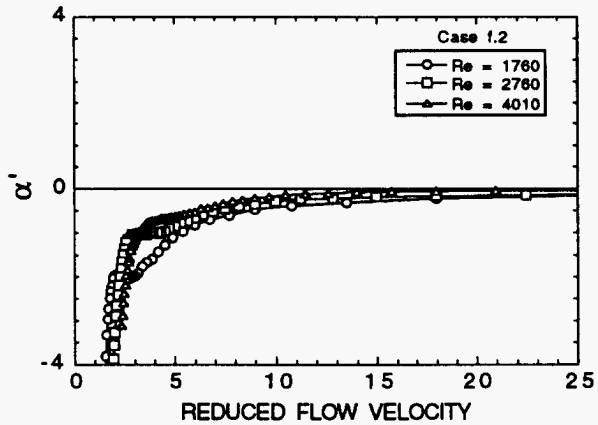
Case f.2
Re = 1760
Re = 2760
Re = 4010
α'
4
0
-4
0
5
10
15
20
25
REDUCED FLOW VELOCITY

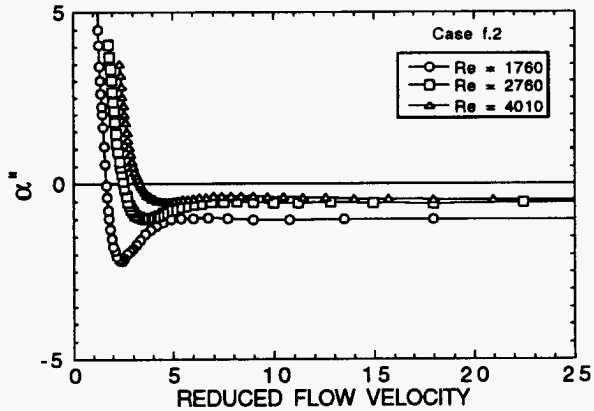
Case f.2
Re = 1760
Re = 2760
Re = 4010
α"
5
0
-5
0
5
10
15
20
25
REDUCED FLOW VELOCITY

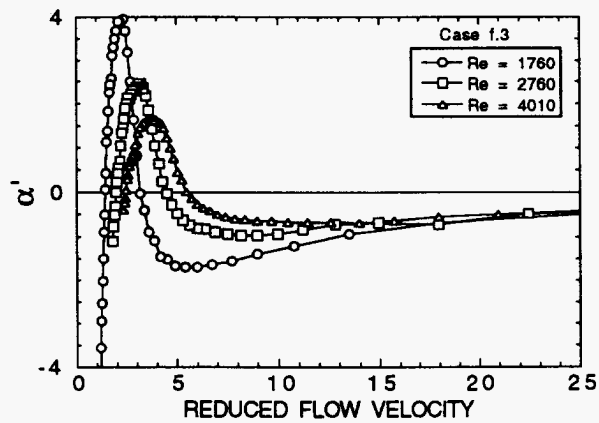
Case f.3
Re = 1760
Re = 2760
Re = 4010
α'
4
0
-4
0
5
10
15
20
25
REDUCED FLOW VELOCITY

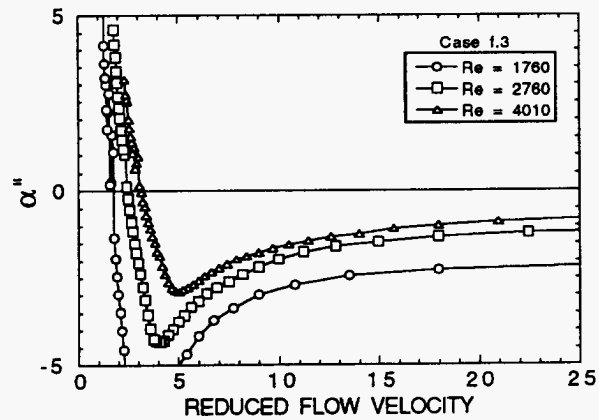
Case f.3
Re = 1760
Re = 2760
Re = 4010
α"
5
0
-5
0
5
10
15
20
25
REDUCED FLOW VELOCITY

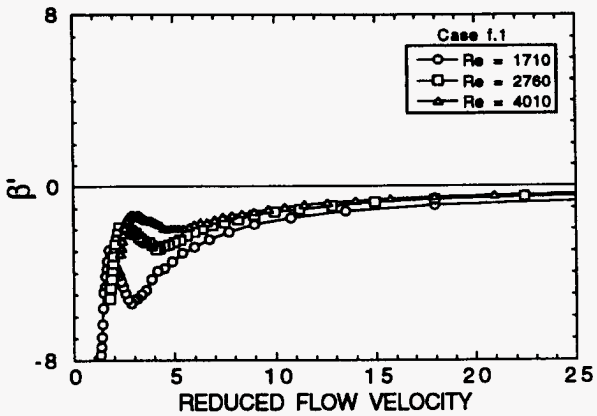
Case f.1
Re = 1710
Re = 2760
Re = 4010
β'
8
0
-8
0
5
10
15
20
25
REDUCED FLOW VELOCITY

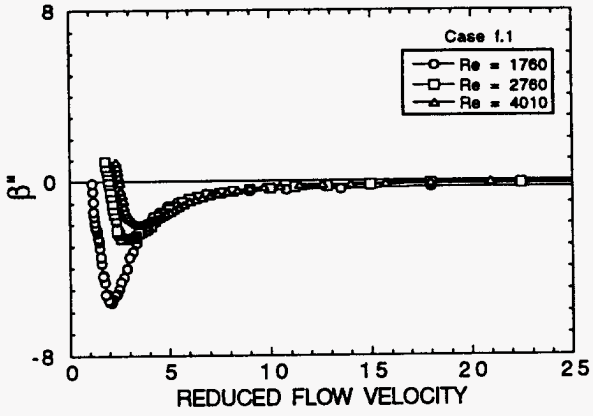
Case f.1
Re = 1760
Re = 2760
Re = 4010
β"
8
0
-8
0
5
10
15
20
25
REDUCED FLOW VELOCITY

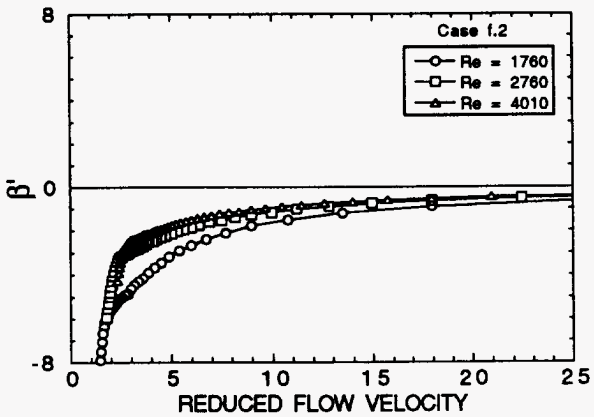
Case f.2
Re = 1760
Re = 2760
Re = 4010
β'
8
0
-8
0
5
10
15
20
25
REDUCED FLOW VELOCITY

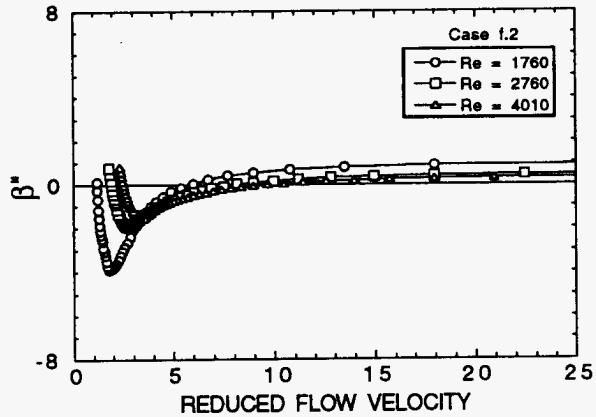
Case f.2
Re = 1760
Re = 2760
Re = 4010
β"
8
0
-8
0
5
10
15
20
25
REDUCED FLOW VELOCITY

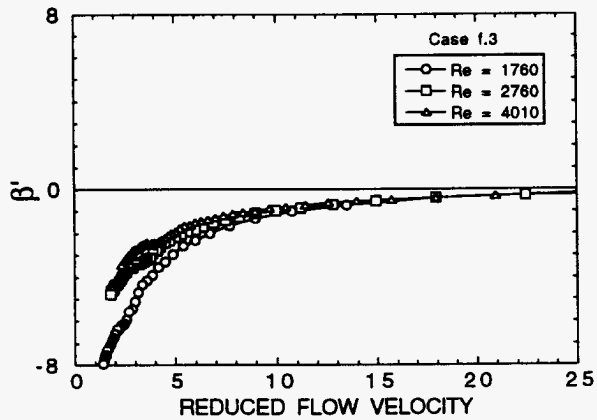
Case f.3
Re = 1760
Re = 2760
Re = 4010
β'
8
0
-8
0
5
10
15
20
25
REDUCED FLOW VELOCITY

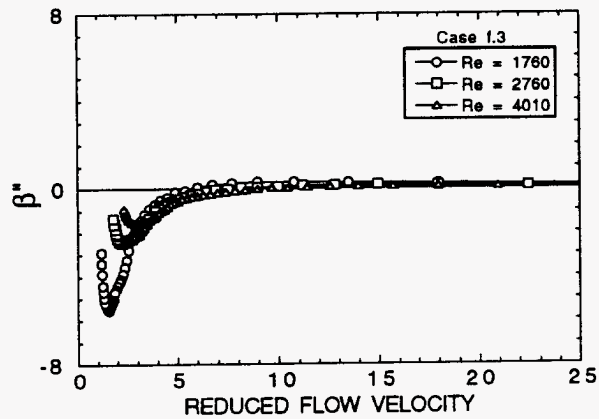
Case f.3
Re = 1760
Re = 2760
Re = 4010
β"
8
0
-8
0
5
10
15
20
25
REDUCED FLOW VELOCITY

F.7.5b

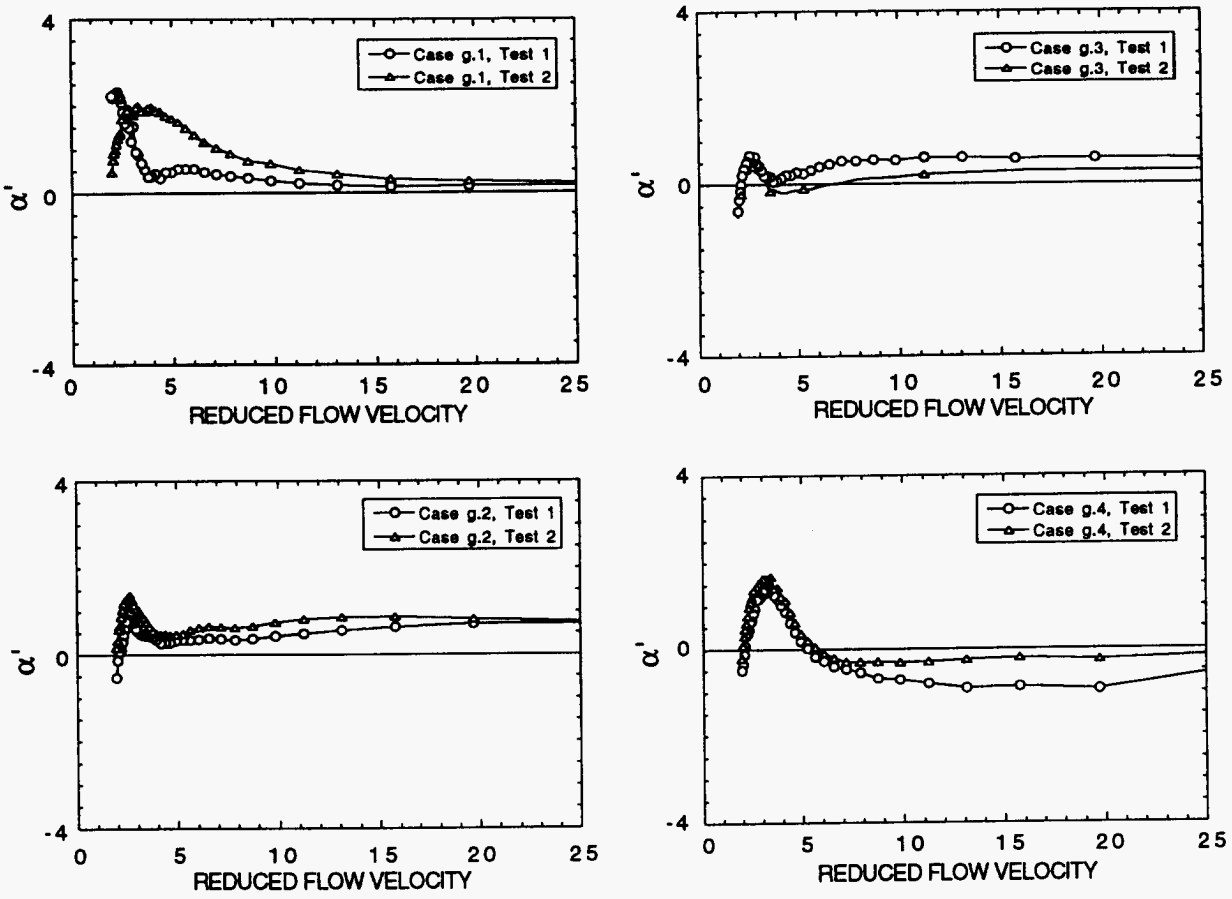
Case g.1, Test 1
Case g.1, Test 2
Case g.3, Test 1
Case g.3, Test 2
Case g.2, Test 1
Case g.2, Test 2
Case g.4, Test 1
Case g.4, Test 2
α'
REDUCED FLOW VELOCITY
4
0
-4
0
5
10
15
20
25

Fig. 6a

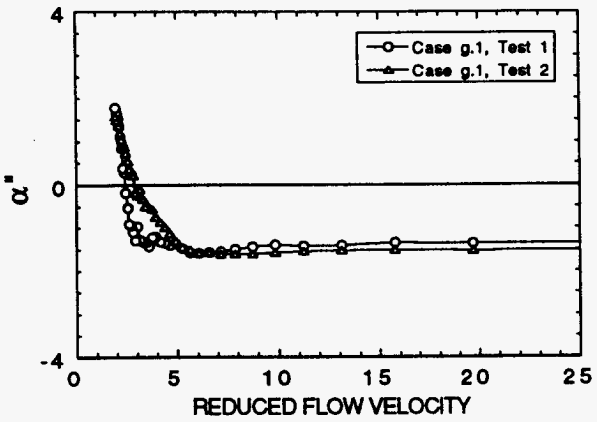
Case g.1, Test 1
Case g.1, Test 2
α"
4
0
-4
0
5
10
15
20
25
REDUCED FLOW VELOCITY

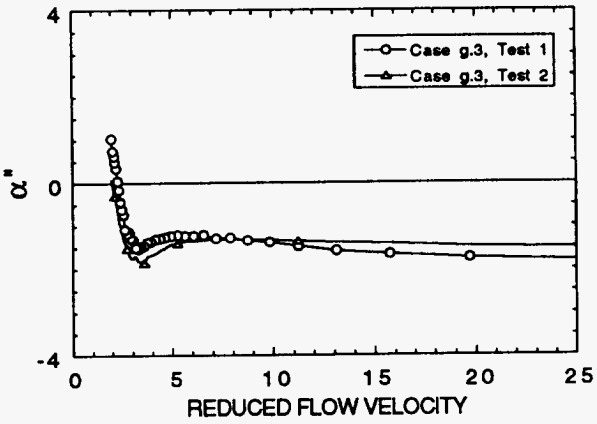
Case g.3, Test 1
Case g.3, Test 2
α"
4
0
-4
0
5
10
15
20
25
REDUCED FLOW VELOCITY

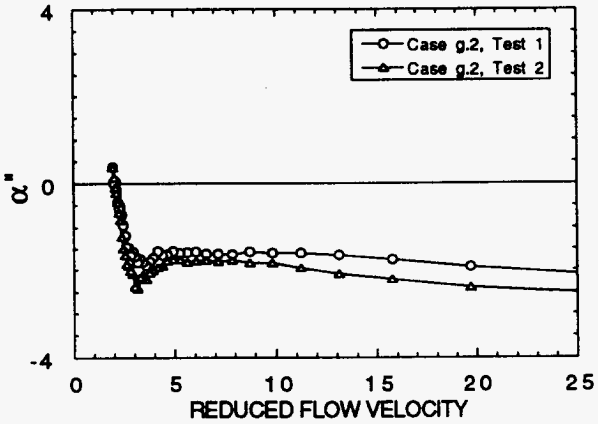
Case g.2, Test 1
Case g.2, Test 2
α"
4
0
-4
0
5
10
15
20
25
REDUCED FLOW VELOCITY

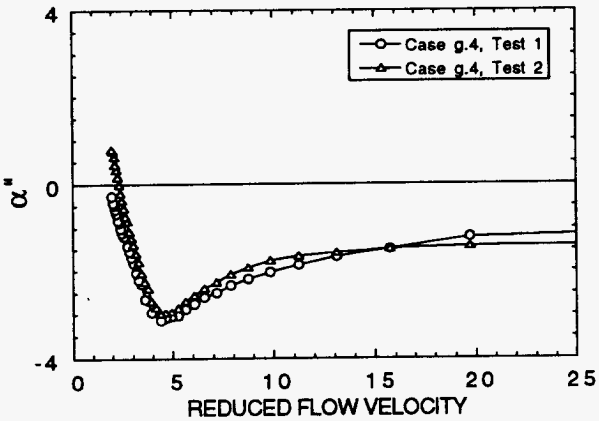
Case g.4, Test 1
Case g.4, Test 2
α"
4
0
-4
0
5
10
15
20
25
REDUCED FLOW VELOCITY

Fig. 5c

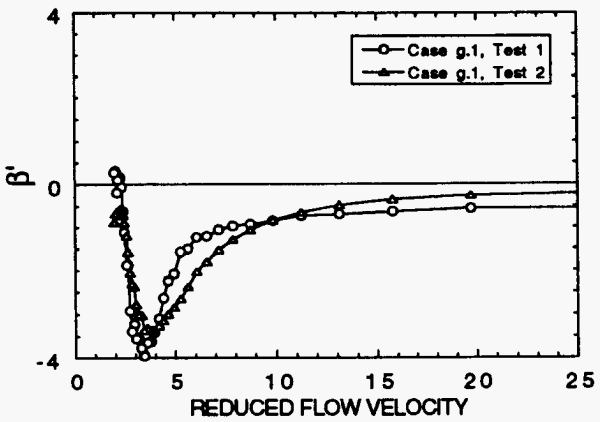
Case g.1, Test 1
Case g.1, Test 2
β'
4
0
-4
0
5
10
15
20
25
REDUCED FLOW VELOCITY

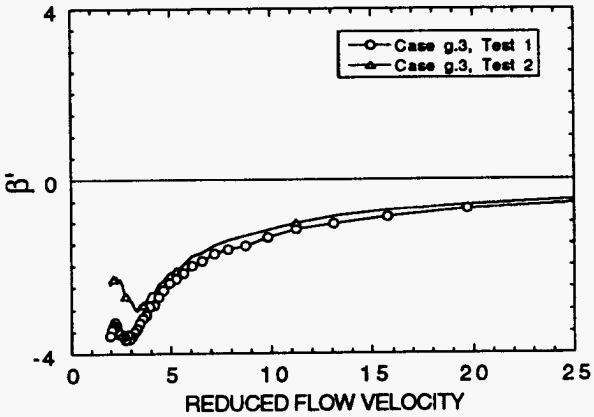
Case g.3, Test 1
Case g.3, Test 2
β'
4
0
-4
0
5
10
15
20
25
REDUCED FLOW VELOCITY

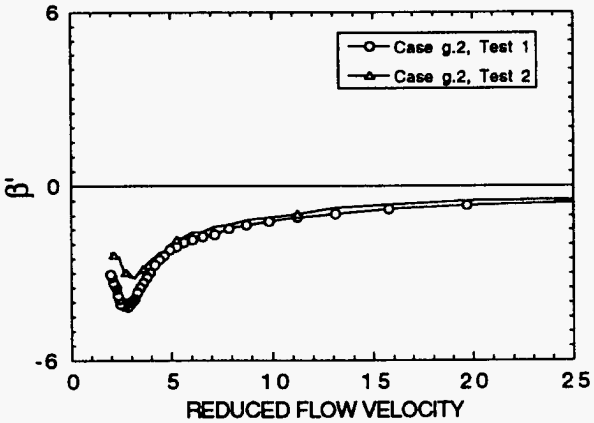
Case g.2, Test 1
Case g.2, Test 2
β'
6
0
-6
0
5
10
15
20
25
REDUCED FLOW VELOCITY

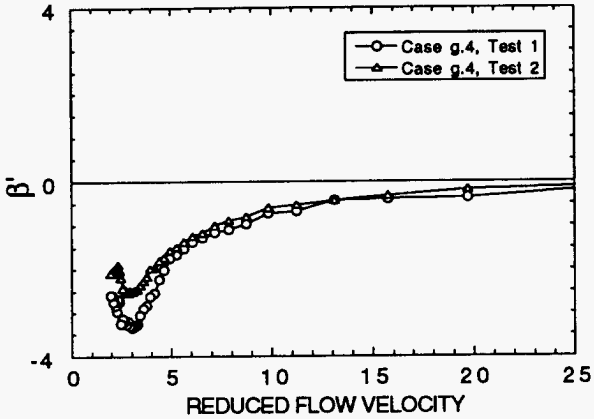
Case g.4, Test 1
Case g.4, Test 2
β'
4
0
-4
0
5
10
15
20
25
REDUCED FLOW VELOCITY

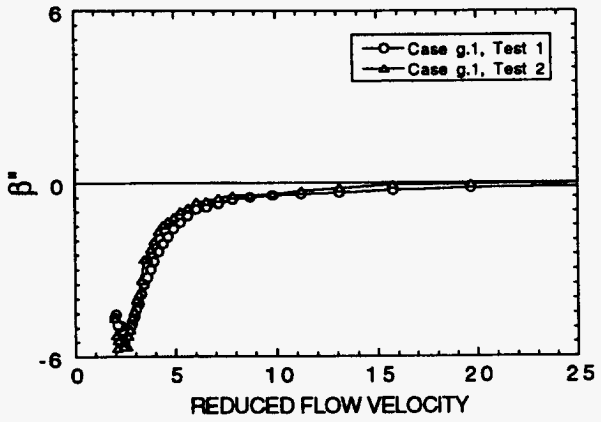
Case g.1, Test 1
Case g.1, Test 2
β"
6
0
-6
0
5
10
15
20
25
REDUCED FLOW VELOCITY

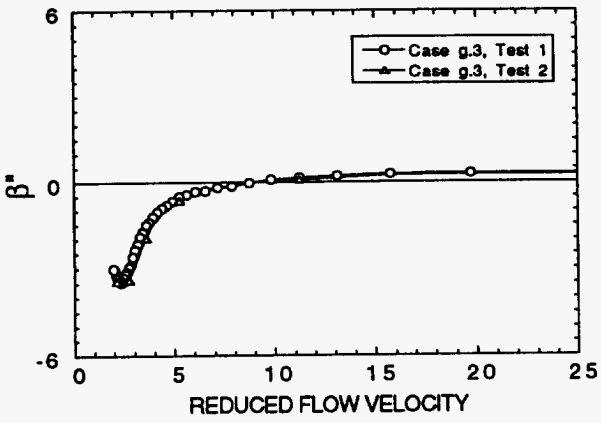
Case g.3, Test 1
Case g.3, Test 2
β"
6
0
-6
0
5
10
15
20
25
REDUCED FLOW VELOCITY

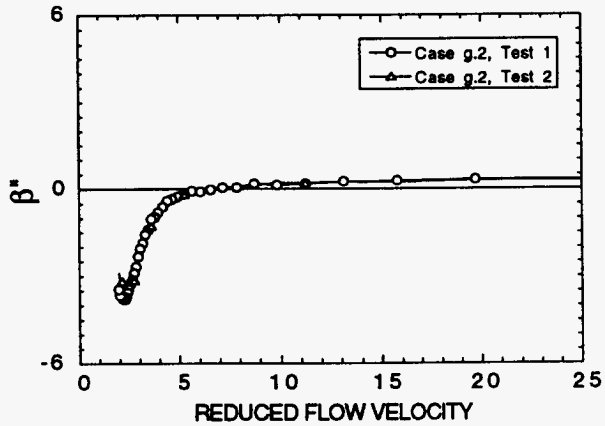
Case g.2, Test 1
Case g.2, Test 2
β"
6
0
-6
0
5
10
15
20
25
REDUCED FLOW VELOCITY

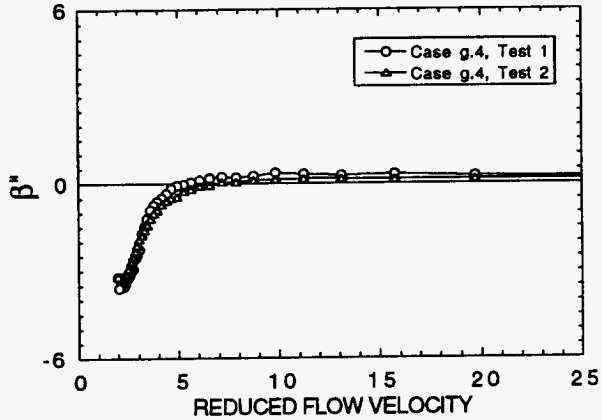
Case g.4, Test 1
Case g.4, Test 2
β"
6
0
-6
0
5
10
15
20
25
REDUCED FLOW VELOCITY

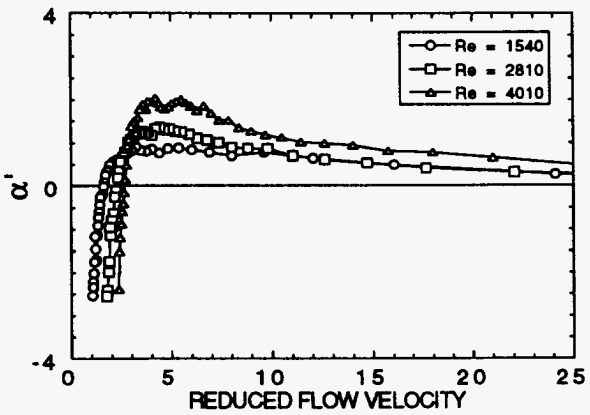
Re = 1540
Re = 2810
Re = 4010
α'
REDUCED FLOW VELOCITY

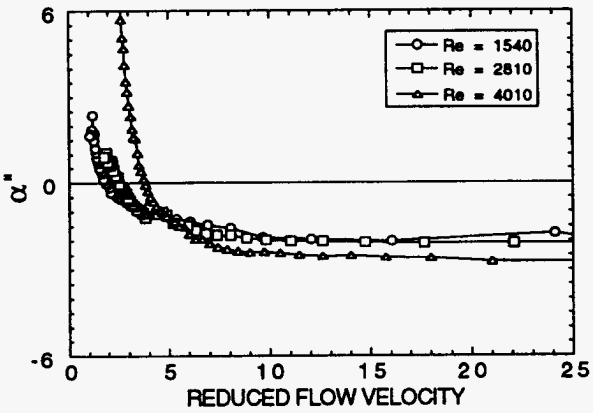
Re = 1540
Re = 2810
Re = 4010
α"
REDUCED FLOW VELOCITY

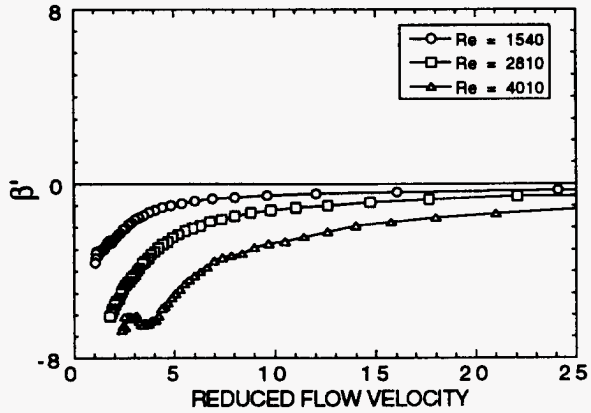
Re = 1540
Re = 2810
Re = 4010
β'
REDUCED FLOW VELOCITY

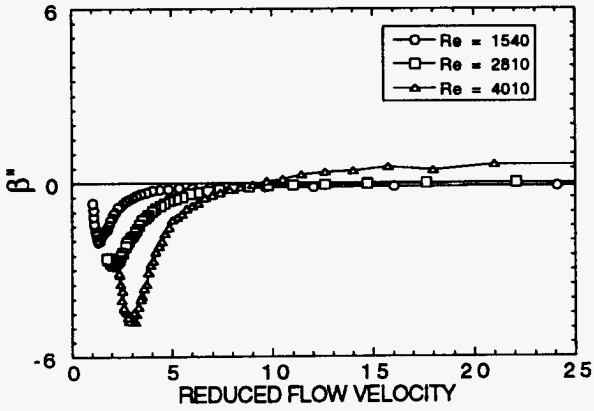
Re = 1540
Re = 2810
Re = 4010
β"
REDUCED FLOW VELOCITY

Fig. 12

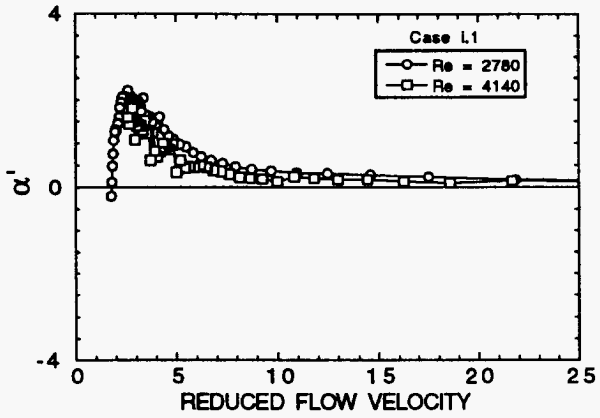
Case I.1
Re = 2780
Re = 4140
α'
4
0
-4
0 5 10 15 20 25
REDUCED FLOW VELOCITY

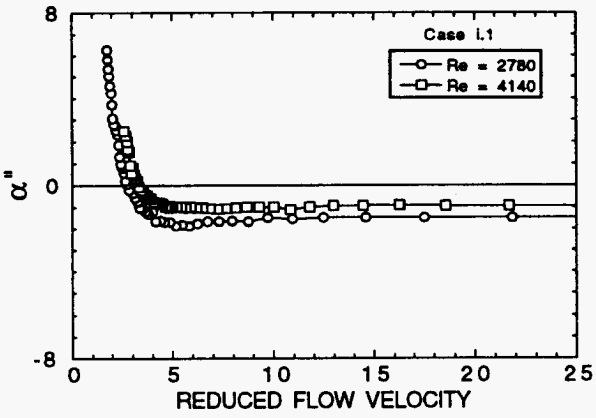
Case I.1
Re = 2780
Re = 4140
α"
8
0
-8
0 5 10 15 20 25
REDUCED FLOW VELOCITY

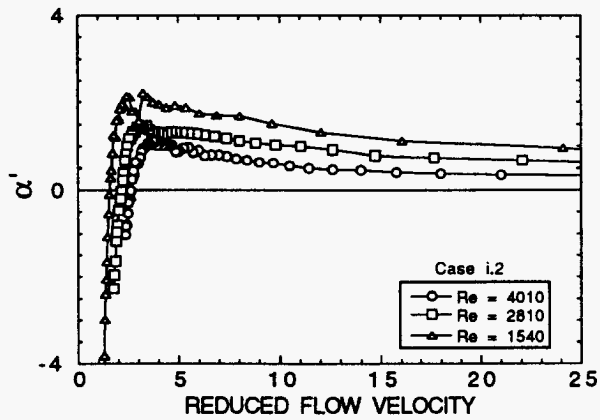
Case I.2
Re = 4010
Re = 2810
Re = 1540
α'
4
0
-4
0 5 10 15 20 25
REDUCED FLOW VELOCITY

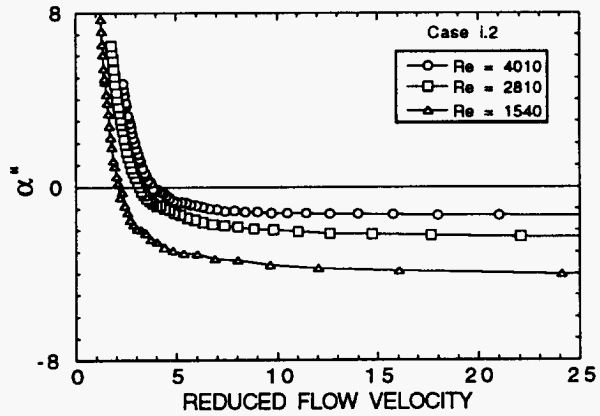
Case I.2
Re = 4010
Re = 2810
Re = 1540
α"
8
0
-8
0 5 10 15 20 25
REDUCED FLOW VELOCITY

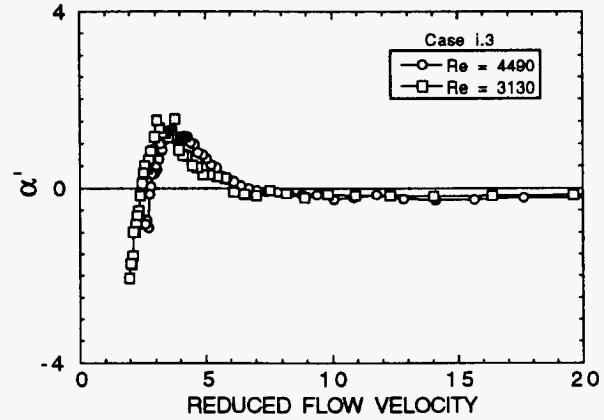
Case I.3
Re = 4490
Re = 3130
α'
4
0
-4
0 5 10 15 20
REDUCED FLOW VELOCITY

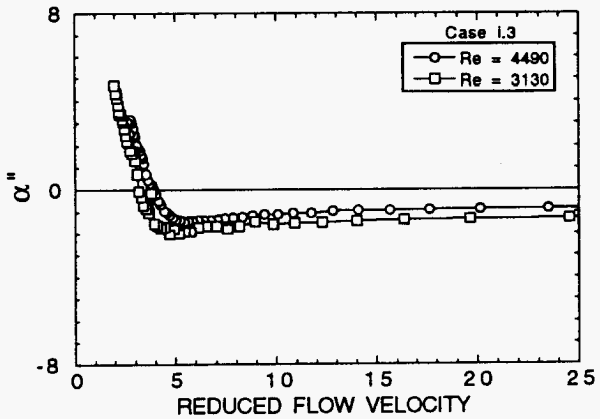
Case I.3
Re = 4490
Re = 3130
α"
8
0
-8
0 5 10 15 20 25
REDUCED FLOW VELOCITY

Fig. 5a

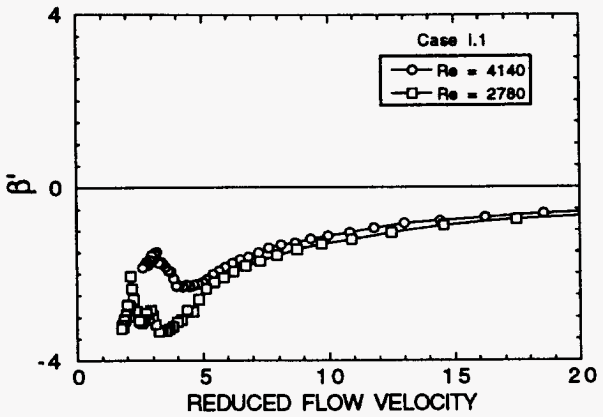
Case I.1
Re = 4140
Re = 2780
β'
4
0
-4
0
5
10
15
20
REDUCED FLOW VELOCITY

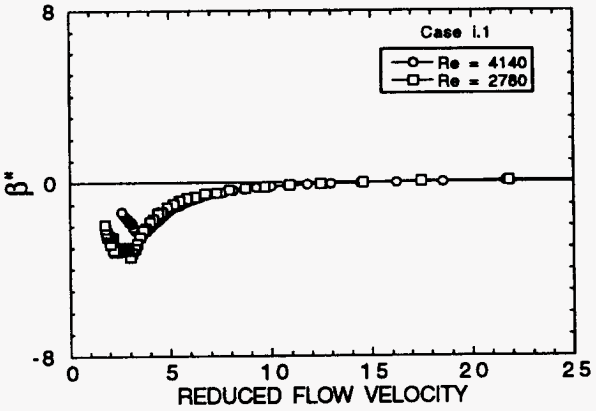
Case I.1
Re = 4140
Re = 2780
β"
8
0
-8
0
5
10
15
20
25
REDUCED FLOW VELOCITY

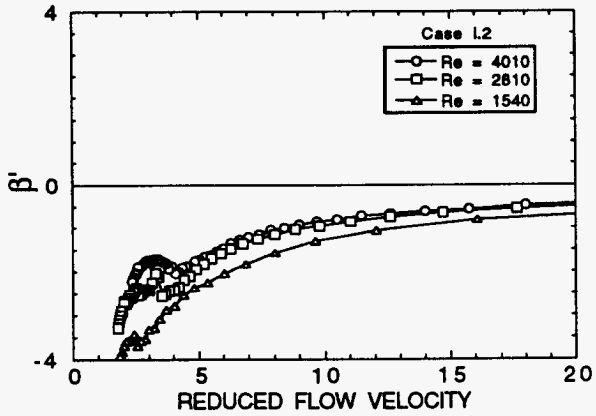
Case I.2
Re = 4010
Re = 2810
Re = 1540
β'
4
0
-4
0
5
10
15
20
REDUCED FLOW VELOCITY

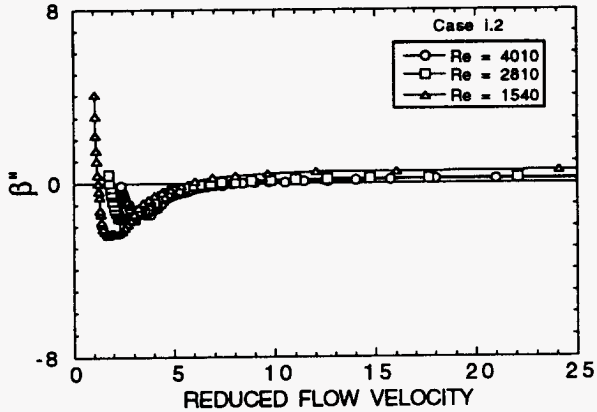
Case I.2
Re = 4010
Re = 2810
Re = 1540
β"
8
0
-8
0
5
10
15
20
25
REDUCED FLOW VELOCITY

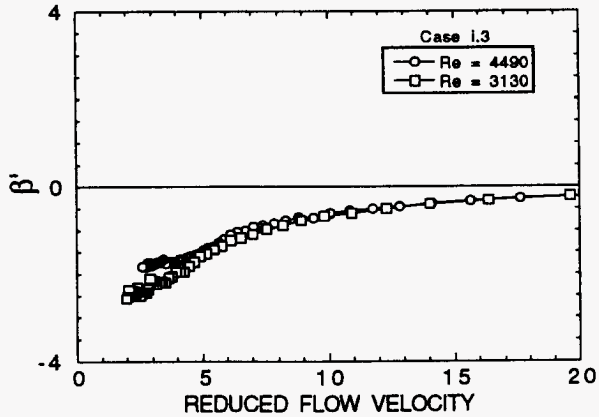
Case I.3
Re = 4490
Re = 3130
β'
4
0
-4
0
5
10
15
20
REDUCED FLOW VELOCITY

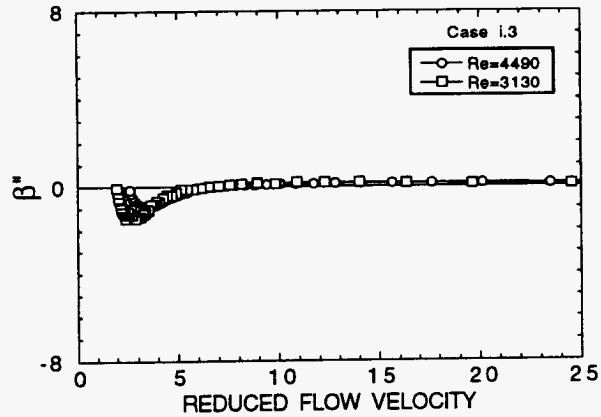
Case I.3
Re=4490
Re=3130
β"
8
0
-8
0
5
10
15
20
25
REDUCED FLOW VELOCITY

Fig. 15b

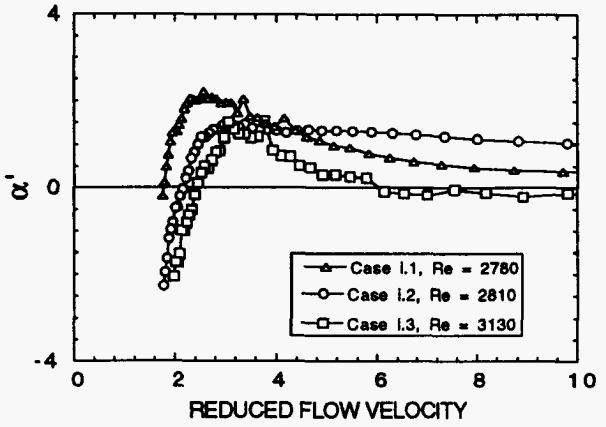
4
0
-4
α'
0
2
4
6
8
10
REDUCED FLOW VELOCITY
Case I.1, Re = 2780
Case I.2, Re = 2810
Case I.3, Re = 3130

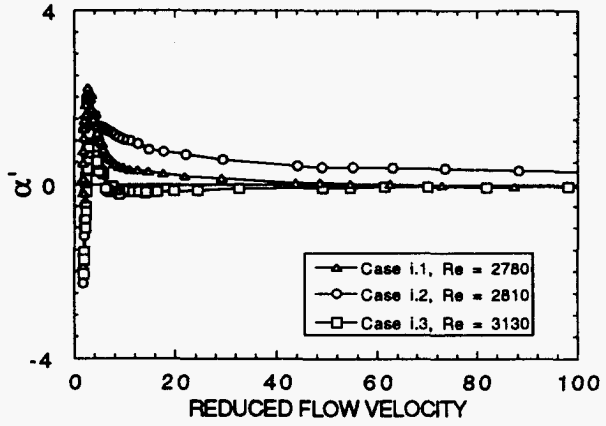
4
0
-4
α'
0
20
40
60
80
100
REDUCED FLOW VELOCITY
Case I.1, Re = 2780
Case I.2, Re = 2810
Case I.3, Re = 3130

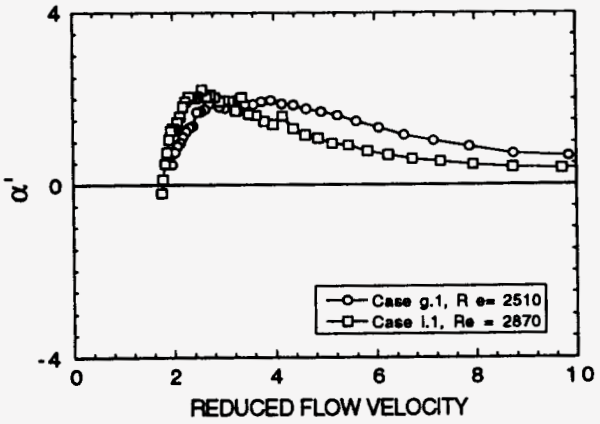
α'
4
0
-4
0
2
4
6
8
10
REDUCED FLOW VELOCITY
Case g.1, R e= 2510
Case I.1, Re = 2870

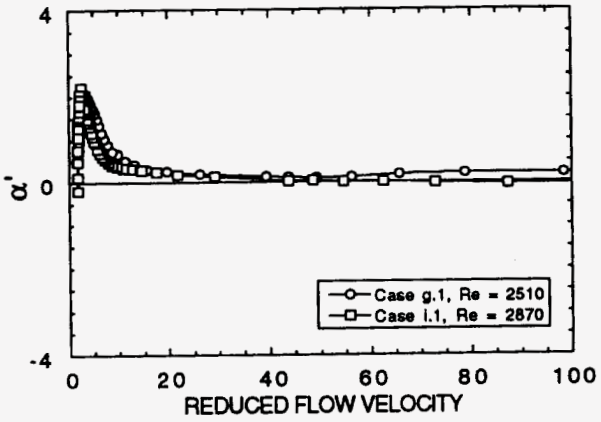
α'
4
0
-4
0
20
40
60
80
100
REDUCED FLOW VELOCITY
Case g.1, Re = 2510
Case I.1, Re = 2870

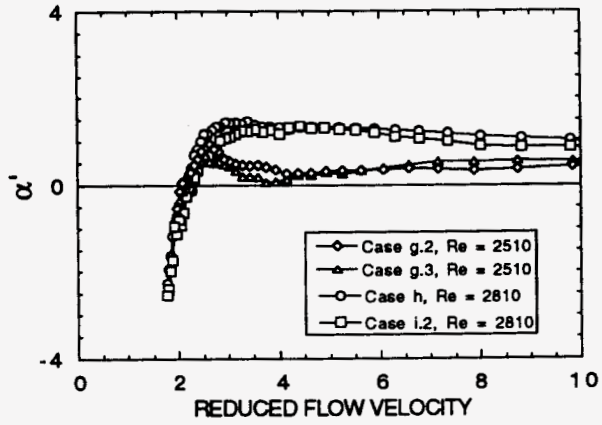
α'
4
0
-4
0
2
4
6
8
10
REDUCED FLOW VELOCITY
Case g.2, Re = 2510
Case g.3, Re = 2510
Case h, Re = 2810
Case I.2, Re = 2810

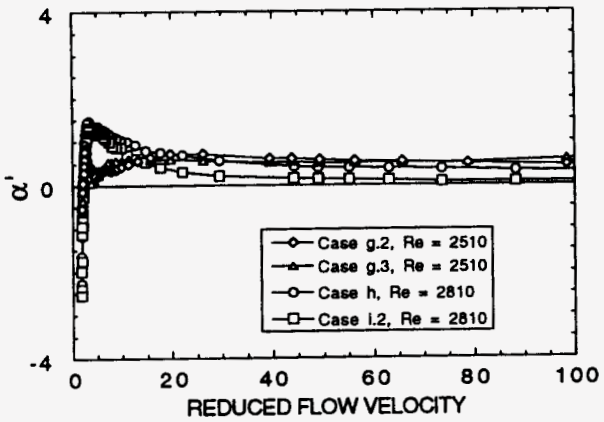
α'
4
0
-4
0
20
40
60
80
100
REDUCED FLOW VELOCITY
Case g.2, Re = 2510
Case g.3, Re = 2510
Case h, Re = 2810
Case I.2, Re = 2810

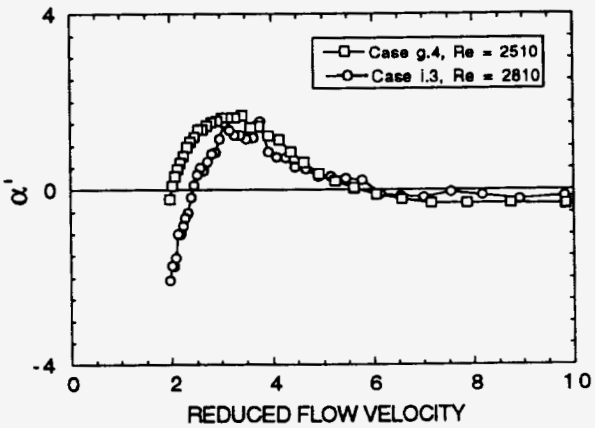
α'
4
0
-4
0
2
4
6
8
10
REDUCED FLOW VELOCITY
Case g.4, Re = 2510
Case I.3, Re = 2810

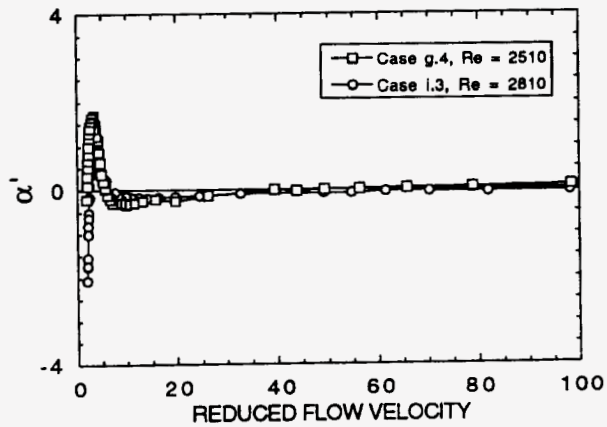
α'
4
0
-4
0
20
40
60
80
100
REDUCED FLOW VELOCITY
Case g.4, Re = 2510
Case I.3, Re = 2810

Fig 7

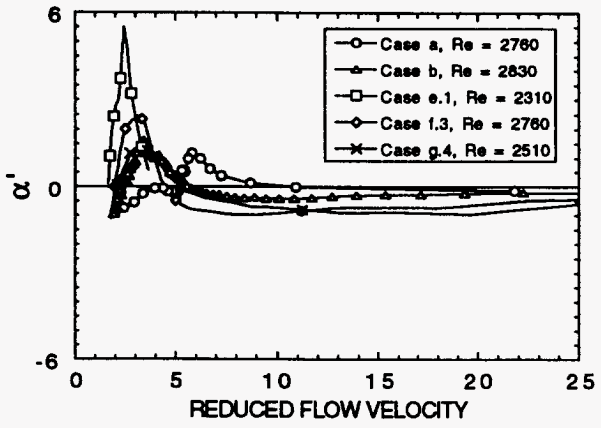
Case a, Re = 2760
Case b, Re = 2830
Case e.1, Re = 2310
Case f.3, Re = 2760
Case g.4, Re = 2510
α'
6
0
-6
0
5
10
15
20
25
REDUCED FLOW VELOCITY

Fig. 18

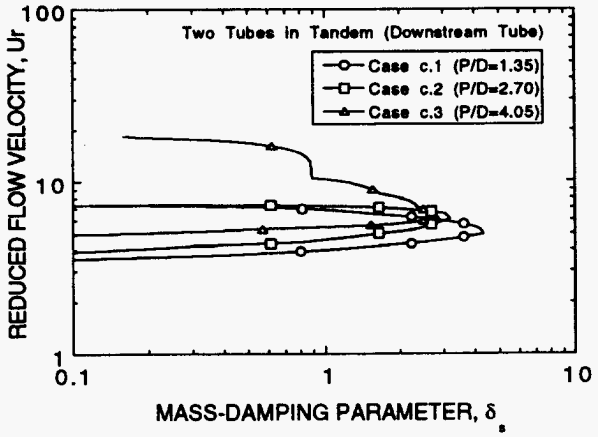
Two Tubes in Tandem (Downstream Tube)
Case c.1 (P/D=1.35)
Case c.2 (P/D=2.70)
Case c.3 (P/D=4.05)
REDUCED FLOW VELOCITY, Ur
100
10
1
0.1
1
10
MASS-DAMPING PARAMETER, δs

Fig. 7

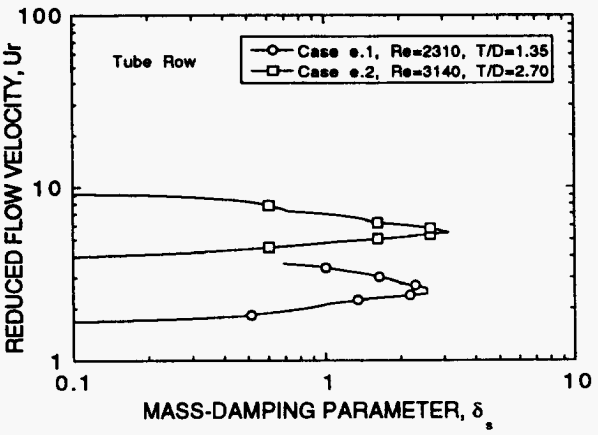
100
10
1
0.1
1
10
REDUCED FLOW VELOCITY, Ur
MASS-DAMPING PARAMETER, δ_s
Tube Row
Case e.1, Re=2310, T/D=1.35
Case e.2, Re=3140, T/D=2.70

Fig. 30

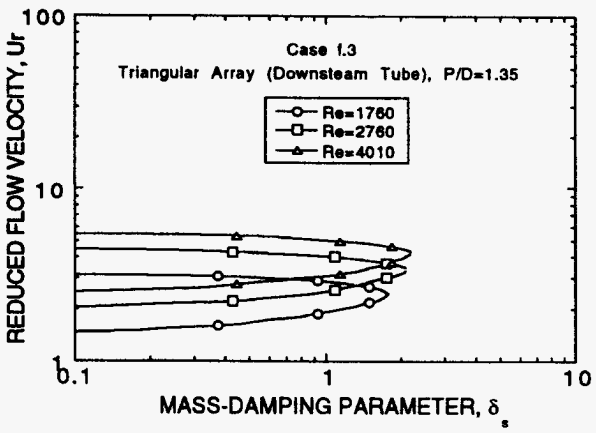
Case 1.3
Triangular Array (Downsteam Tube), P/D=1.35
Re=1760
Re=2760
Re=4010
REDUCED FLOW VELOCITY, Ur
100
10
1
0.1
1
10
MASS-DAMPING PARAMETER, δs

Fig. 21

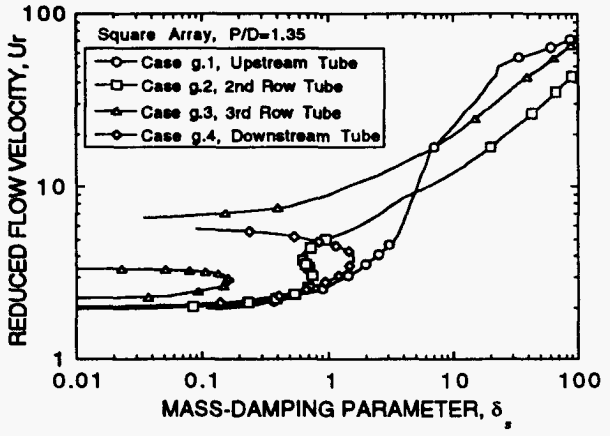
Square Array, P/D=1.35
Case g.1, Upstream Tube
Case g.2, 2nd Row Tube
Case g.3, 3rd Row Tube
Case g.4, Downstream Tube
REDUCED FLOW VELOCITY, Ur
100
10
1
0.01
0.1
1
10
100
MASS-DAMPING PARAMETER, δ_s

Fig. 22

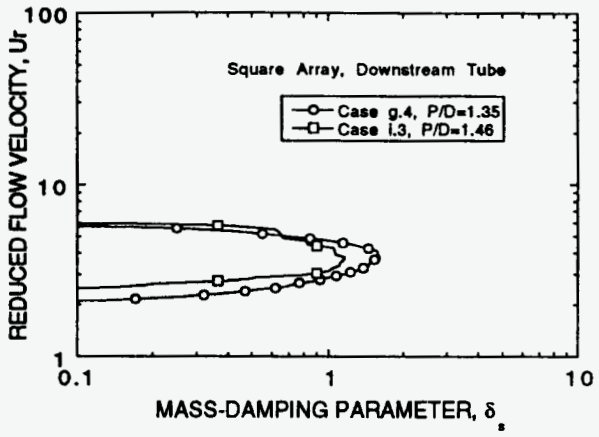
Square Array, Downstream Tube
Case g.4, P/D=1.35
Case i.3, P/D=1.46
REDUCED FLOW VELOCITY, Ur
100
10
1
0.1
1
10
MASS-DAMPING PARAMETER, δs

Fig. 23

Report Number (14) ANL/ET/CP--92179
CONF-971115--

Publ. Date (11) 199708
Sponsor Code (18) EPRI, XF
UC Category (19) UC-000, DOE/ER

DOE